MULTIPLE LINEAR REGRESSION MODELS FOR THE ESTIMATION OF PH AND ARAGONITE SATURATION STATE IN THE NORTHWESTERN GULF OF MEXICO

A Thesis

by

EVALYNN PATRICIA JUNDT

B.S., Bemidji State University, 2020

Submitted in Partial Fulfillment of the Requirements for the Degree of

MASTER OF SCIENCE

in

COASTAL AND MARINE SYSTEM SCIENCE

Texas A&M University-Corpus Christi
Corpus Christi, Texas

August 2022

August 2022

MULTIPLE LINEAR REGRESSION MODELS FOR THE ESTIMATION OF PH AND ARAGONITE SATURATION STATE IN THE NORTHWESTERN GULF OF MEXICO

A Thesis

by

EVALYNN PATRICIA JUNDT

This thesis meets the standards for scope and quality of
Texas A&M University-Corpus Christi and is hereby approved.

Xinping Hu, PhD
Chair

C. Liu, PhD
Committee Member

L. Jin, PhD
Committee Member

August 2022

ABSTRACT

The ocean plays a vital role in making up 70% of the Earth's surface, producing over half of oxygen globally, and absorbing approximately 30% of anthropogenic CO_2 since the industrial revolution. Ocean acidification (OA) is a direct threat to many organisms living in the oceans across the globe, yet the state of carbonate chemistry and the rate of OA vary in different parts of the world's oceans. Although current data suggest that the open Gulf of Mexico (GOM) surface waters have relatively high pH (> 8) and aragonite saturation state ($\Omega_{Arag} > 3$), the GOM could still experience ecological impacts of OA. In addition, the combination of increasing atmospheric CO_2, upwelling, and increasing terrestrial nutrient export may acidify the coastal waters even further.

Acidifying ocean waters have decreasing Ω_{Arag}, posing serious threats to calcifying organisms, affecting their populations, growth patterns, and shell or skeletal density. The GOM is home to the northernmost tropical coral reefs around the contiguous United States as well as prominent shellfish industry. Historical water column carbonate measurements are scarce, so the progression of OA in the GOM is poorly understood. Research regarding OA in the GOM is needed to manage and protect these resources. In the literature, multiple linear regression (MLR) models have been created to fill data gaps in different ocean regions such as the Gulf of Alaska, the Southern Ocean, the Sea of Japan, and coasts of the northeastern and northwestern United States. Prior to this study, no statistical model existed for carbonate chemistry parameters (i.e., pH and Ω_{Arag}) in the GOM. By creating models built upon the relationships between commonly measured hydrographic properties (salinity, temperature, pressure, and dissolved oxygen (DO))

and pH as well as Ω_{Arag}, data gaps can be filled in areas that do not have sufficient sampling coverage.

In this study, I created statistical models for the estimation of Ω_{Arag} and pH in the northwestern GOM (NWGOM) from latitudes 27.1-29.0˚N and longitudes 91.5-95.0˚W. The calibration data used in the models include depth, salinity, temperature, pressure, and DO collected from four cruises that took place in July 2007, July 2017, and April and August of 2021. The models predict Ω_{Arag} with $R^2 \geq 0.98$, RMSE ≤ 0.14 and pH with $R^2 \geq 0.93$, RMSE $\leq$ 0.02 for four different subsets of the data depending on depth (with and without removal of upper 20 m) and geographic location (with and without removal of stations to the east).

The data used to create the models are also used to create contour plots that show variation of Ω_{Arag} and pH over the timeframe of the study from 2007 to 2021. Relatively low Ω_{Arag} ($\Omega_{Arag} \leq 2$) values are present in the depths $\geq$ 180 m. The depth range of the water column between Ω_{Arag} = 2-1.5 decreased over this period. The depths for $\Omega_{Arag} = 2$ and $\Omega_{Arag} = 1.1$ vary ±20 and ±50 m respectively, while the depth for $\Omega_{Arag} = 1.5$ decreased 50 m from 2007 to 2021. Depth profiles for pH revealed consistent patterns over all four cruises with highest values over the shelf and upper 125 m, and minimum values around 500 m. The pH = 7.9 isopleth remained around 265 m for all cruises, while the pH = 8 isopleth showed fluctuation of ±10 m (from 2007 to 2021). On the shelf, the maximum and minimum pH values were 0.0356 and 0.0133 units lower in 2021 than in 2007, respectively. This resulted in the range of pH values experienced narrowing by 0.0223 and transitioning to lower pH values overall.

These MLR models are valuable tools for reconstructing Ω_{Arag} and pH data where direct chemical observations are absent but hydrographic information is available. These models can be applied to the NWGOM within ±10 years of 2014, although observations of potential shifts in

circulation, water mass composition, and anthropogenic CO_2 should be monitored to improve or revise these models in the future.

ACKNOWLEDGEMENTS

I would like to acknowledge Dr. Xinping Hu who has been my advisor over the last two years and thankfully agreed to continue as my advisor into my doctoral program. I first thank him for seeing enough potential in me to invite me to join the Ecosystem Science and Modeling Lab. I know I gave him quite a shock initially with my “unique” style but nonetheless he has treated me with such great care and provided me with all the opportunities I have needed to grow and succeed. I am particularly grateful he placed enough trust in me to represent him and our lab on the NOAA GOMECC4 cruise which was truly an amazing opportunity that pushed such growth in me as scientist and I never would have had without him. I would have never imagined being able to work in such a wholistic work environment under someone with such great knowledge and phenomenal worth ethic.

I would also like to acknowledge the other members of my committee- Dr. Lei Jin and Dr. Chuntao Liu. Their expertise in statistics and atmospheric sciences helped to provide additional point of views, and knowledge in the interdisciplinary aspects of this study. Both provided much appreciated help with crossdisciplinarity language intricacies as well as numerous points of improvement which would never have been thought of without the diversity of knowledge they have.

I am additionally grateful for the support and hard work of all lab members present and past. C.J. Staryk provided me with hours of training on lab equipment as well as field sampling. Additionally, he has been a major contributor to the processing of the samples for this study. I have shared office space with Larissa Dias for the entirety of my time and she has shared much great advice and fellowship over the years. I also shared office space with Nicole Kumbula and

Christian Amos for the second half of my time and they both provided great company, conversation, and collected and analyzed many samples for this study. Mellissa McCutcheon left shortly after my starting but in that time provided ample advice and training.

Thanks to the Harte Research Institute at Texas A&M University- Corpus Christi for providing the wonderful office and lab space to Dr. Xinping Hu's lab that were used during this project. Additional thanks for funding my Research Assistantship position which helped support me over this time period.

Above all, the greatest acknowledgement needs to go to my family for all of the love and support over the years. To my pets who never stop supporting me in anything and everything I do. To my friends and extended family who watched and offered words of encouragement. To my grandparents who always jumped on the chance to encourage me and offer to do and give far too much to support me. To my siblings whose admiration has always pushed me to be stronger, go farther and do better in example. To my parents PattiLynn, Ed and Denise who spent so many years guiding me and teaching me to direct my fire and passion in the proper way to pursue and achieve my dreams. To my husband Steven who deserves a degree or award of his own for supporting me, being my best friend and comforter through all the trials of life, especially graduate school.

TABLE OF CONTENTS

LIST OF FIGURES

LIST OF TABLES

CHAPTER I. INTRODUCTION

I.1 Anthropogenic CO_2 buildup and ocean acidification

Ocean acidification (OA) has become a household name in the discussion of climate change. OA caused by the uptake of atmospheric CO_2 results in a reduction in both pH (i.e., increase in acidity) and carbonate saturation state, along with its biological and ecological impacts. These changes in the ocean occur over timescales of decades or longer. The anthropogenic CO_2 in the atmosphere since the preindustrial period is a direct consequence of fossil fuel burning, deforestation, cement production, and other processes. When averaged between 1859-2019, 81% of emissions resulted from fossil fuels (energy and cement production) and 19% from land-use changes. These activities pushed 11.5 ± 0.9 Gt-C yr^{-1} into the atmosphere in 2019 alone (Friedlingstein et al., 2020). Of this influx of anthropogenic CO_2, less than half remains in the atmosphere while the rest is reabsorbed by the land and ocean (Sabine et al., 2004). CO_2 absorbed by the ocean has resulted in pH decrease by 0.1 units since pre-industrial levels, representing a 30% increase in proton concentration (Orr et al., 2005). Studies indicate current pH changes from - 0.0010 to - 0.0068 yr^{-1} with an ultimate 0.4-0.5 unit decrease projected in the "business-as-usual" scenarios by end of this century (García-Ibáñez et al., 2016; Ishida et al., 2021; Orr et al., 2005).

Despite increased awareness of the alarming trends, CO_2 emissions grew at a rate of 1.2% yr^{-1} in the last decade (Friedlingstein et al., 2020). Under these circumstances as the oceanic sink continues to mitigate the buildup of atmospheric CO_2, it will result in continuing acidification and further reductions of pH and carbonate saturation (Ω). This change in pH will be accompanied by an average Revelle Factor increase of 3.7 ± 0.9 from 2000 to 2100 (Jiang et al., 2019). Decreases in pH and buffering capacity thus are expected to cause an acceleration in

acidification and decrease in the ocean's ability to absorb and mitigate further atmospheric CO_2 buildup. It is expected in business-as-usual scenarios there will be an observed pH change of -0.02 units decade^{-1} at the beginning of the century, accelerating toward an average of about -0.04 units decade^{-1} due to decreasing buffer towards the end of the century (Orr et al., 2005, Jiang et al., 2019).

I.2 The marine carbonate system

The capability of oceans to store absorbed CO_2 is attributed to seawater's buffering capability. Through a chain of processes, from dissolution to dissociation, only a small amount of absorbed CO_2 remains undissociated (i.e., aqueous CO_2, or CO_2^*). Due to this reaction, CO_2 invasion into seawater results in changes to the speciation of the carbonate system. Thus, increase in CO_2^* is proportional to the CO_2 increase in the atmosphere however, the increase of total dissolved inorganic carbon (DIC) concentration in the water is lower than that in the atmosphere. This is a result of CO_2 being transformed into other carbonate species (HCO_3^-, CO_3^{2-}) in part by the release of H^+ ions.

$$\Omega_{sp} = [Ca^{2+}][CO_3^{2-}] / K_{sp'} \quad . \qquad (1)$$

In equation (1), $[Ca^{2+}]$ is the concentration of calcium ion, $[CO_3^{2-}]$ is the concentration of carbonate ion, and $K_{sp'}$ is the stoichiometric solubility product (Zeebe and Wolf-Gladrow, 2001). The solubility product is a function of the mineral phase (calcite or aragonite), pressure, salinity, and temperature. Based on thermodynamics, when the value of $\Omega > 1$ (supersaturation), it allows for calcification to occur while values of $\Omega < 1$ (undersaturation) lead to dissolution. Though this varies in real world, experimental studies have shown dissolution and zero net calcification where $\Omega \geq 1$ (Bednarsek et al., 2012; Anthony et al., 2008).

I.3 Effect of OA on marine organisms

The alteration of the carbonate system causes pressing changes, specifically decreasing Ω_{Arag} and pH can lead to unfavorable conditions for calcareous organisms such as corals, shellfish, calcareous algae, and important species on the ocean food chain (such as pteropods) by affecting calcification. Calcification is the process used by calcifying organisms to produce shells, skeleton and exoskeletons, and is necessary for growth and reproduction. Calcifying organisms precipitate calcium carbonate material for their needs using bicarbonate and calcium ions dissolved in the seawater (Equation 2). Calcification can be influenced by size and age of the organism, temperature, pH, salinity, and Ω.

$$Ca^{2+} + 2HCO_3^- \rightarrow CaCO_3 + H_2O + CO_2 \quad . \quad (2)$$

The effects of OA on marine organisms are diverse and still largely unexplored, especially on the ecosystem level and in conjunction with other stressors (such as warming and deoxygenation). Nevertheless, the most common results related to OA in the literature are detrimental. For example, numerous studies have linked OA to deleterious effects on corals, plankton, bivalves, sponges, fishes, and echinoderms (Anthony et al. 2008; Wood et al. 2008; Perry et al., 2013; Schneider and Erez, 2006; Albright et al., 2018). On the other hand, some studies showed that certain species of fish and corals are unaffected by OA (Clark et al., 2020; Comeau et al., 2019), and other species can benefit from the CO_2 enrichment (Zimmerman, 2021; Liu et al., 2020; Takahashi et al., 2016).

Previous studies showed that calcifiers such as corals and some sponges have varied responses to OA by species including bleaching, lower calcification ability, weaker structures, net erosion, and dissolution under OA conditions (Anthony et al. 2008; Wood et al. 2008; Perry et al., 2013; Schneider and Erez, 2006; Albright et al., 2018). Decreased calcification rates can result in distorted energy allocation, lower growth rates, reduced reproductive output, and

decreased survival (Wood et al. 2008). Elevated CO_2 can act as a bleaching agent for corals and crustose coralline algae (Anthony et al. 2008). Vulnerability to these effects may be increased in larval organisms as well as organisms using the more soluble form of carbonate, i.e., aragonite. Caribbean corals at current CO_2 levels have shown a 50% reduction in carbonate production since the Holocene and 30% of sites had even become net erosional (Perry et al., 2013). A study on *Acropora eurystoma* showed a 30% decrease in carbonate concentration, equivalent to approximately 0.2 pH units decrease in seawater, caused a calcification rate decrease of 50% (Schneider and Erez, 2006). Other studies have shown that a decrease of Ω_{Arag} by 0.79± 0.03 $\mu mol \cdot kg^{-1}$ from a background value of 3.70± 0.08 to 2.91 ± 0.08 $\mu mol \cdot kg^{-1}$ causes a 34% decrease in net community production in a semi enclosed Australian lagoon (Albright et al., 2018). Even at supersaturated Ω_{Arag} between 1.5-2, crustose coralline algae already exhibit net dissolution (Anthony et al., 2008).

Although the chief concern of OA lies with calcifiers, non-calcifying organisms are not immune to the effects of OA and whole ecosystems may experience changes. Decreases in pH or CO_2 partial pressure (pCO_2) have been observed increasing late-stage loss of embryos in squid species and affecting the biochemical composition of seaweed species (Velez et al., 2021; Zakroff and Mooney, 2020). Studies have documented correlation between pH and the size of otoliths developed in clownfish larvae (Munday et al., 2011b). Although direct threats to the survival of non-calcifying species have not been widely reported (Munday et al., 2011a; Porzio et al., 2011), these findings may be indicative of other unstudied changes with potentially detrimental effects.

With impacts reaching from species to kingdoms, the effects on entire ecosystems will no longer be exclusively an environmental loss but an economic loss as well. It is predicted that the

variability in responses of corals and sponges will lead to vast differences in the assemblages seen in the future. As coral reefs may become dominated by small robust species, deep-water sponge populations in the Gulf of Mexico (GOM) could also see a changes in dominant species and cover (Goodwin et al., 2014; Madin et al., 2008). Studies have shown speciation and coral cover to be significantly and positively correlated with coral reef fish species diversity and abundance (Bell and Galzin, 1984; Komyakova et al., 2013). Predicted decreased calcification, speciation, and cover of corals will likely negatively impact reef fish populations.

The impact of OA on calcifying organisms could total up to significant costs to the marine ecosystem. Reefs provide ecosystem services protecting coasts from hurricanes, erosion, and waves. The reefs also provide tourism, recreational and commercial fishing in adjacent waters. Although economic values specific to the GOM are scarce, in 2007 the total primary value of US commercial fishing harvests was nearly $4 billion, of which 49% came from calcifying organisms alone (19% mollusks and 30% crustaceans) and an additional 24% from fishes that feed directly on calcifying organisms (Narita et al., 2012). Commercial fish processing and wholesaling also supported 63,000 jobs in the same year (Cooley & Doney, 2009). Although data predicting the impact of OA on populations of many species is minimal or entirely missing, data for mollusks predict decreases in yield between 35%-43% translating to a $400 million dollar loss per year (Narita et al., 2012). In addition to future economic losses due to declining populations, currently 80%-85% of oyster reef habitats and 50% of coral habitats have been lost over the last 130 years and projected costs to repair damaged reefs is between $52,000-$260,000 and $6,000-$4,000,000 USD per hectare respectively (Beck et al. 2011; Grabowski et al. 2012; Bayraktarov et al., 2019).

I.4 Hydrography of the GOM

The surface circulation and variability in the GOM is primarily dominated by the Loop Current and its ring separations, while the coastal waters are influenced by freshwater inputs, wind, and upwelling (Sturges and Leben, 2000; Oey et al., 2005). Loop Current intrusion varies temporally. The influence of Loop Current eddies in the northwestern GOM (NWGOM) is less likely to occur in autumn and winter and more likely to occur in spring and summer. In summer, the Loop Current can intrude as far as ~28°N and 90.5°W (Delgado et al., 2019). The Loop Current and its rings contain water with physical and chemical properties that differ from ambient seawater. When ring separations occur, they persist until complete transformation into Gulf Common Water occurs on the western slope of the GOM where the Loop Current eddies break and mix with the surrounding seawater (Vidal et al., 1992, 1994).

Circulation variability in the GOM, in addition to the effects of the Loop Current and ring separations, is attributed to the Mississippi-Atchafalaya River System. Due to this influence, NWGOM may be susceptible to changes in enhanced hydrological cycles (Huang et al. 2015). The Mississippi-Atchafalaya River system influences the upper 50 m of the water column with low salinity waters found hundreds of kilometers from its discharge zone, above the 26 $kg \cdot m^{-3}$ isopycnal (Morey et al., 2003; Jochens and DiMarco, 2008; Portela et al., 2018). The spatial effect of this river system is dependent on the seasonal freshwater budget, heat fluxes, and wind stress (Morey et al., 2003; Müller-Karger et al., 2015). Due to global climate change and enhanced hydrological cycles the freshwater budget varies greatly. For example, between 1951 and 2000, the Mississippi River experienced a 31% increase in its cumulative discharge (Milliman et al., 2008). It is predicted that the discharge of the Mississippi will increase an additional 20% under the scenario with doubling atmospheric CO_2 (from around 350 to 700 ppm), which will further increase the frequency of the hypoxic zone by 32% (Milliman et al.,

2008; Miller and Russell, 1992; Rabalais et al., 2009). Expected precipitation increase in the Mississippi-Atchafalaya watersheds will cause increased discharge hence terrestrial nutrient export, enhanced shelf water stratification, and summer hypoxia in nearby coastal waters (Cloern, 2001). Recent studies have linked coastal acidification to eutrophication in the Long Island Sound, the East China Sea, and the northern GOM shelf (Wallace et al., 2014; Chou et al., 2013; Cai et al., 2011; Sunda and Cai, 2012), as excess nutrients stimulate algal blooms and the decomposition of the latter in bottom water consumes oxygen and produces CO_2 (Chou et al., 2013; Rabalais et al., 2002; Cai et al., 2011).

I.5 Analytical and model methods for the marine carbonate system

Although OA is quickly increasing in popularity as a research topic, with 76.1% of all publications being in the span from 2013 to 2019, most datasets collected before this time are lacking measurements on the carbonate system (Sahoo and Pandey, 2020). Current spatial and temporal coverage of carbonate chemistry data for the GOM is sparse. Available data that cover large swarth of areas in the Gulf is limited to those obtained from the Gulf of Mexico and East Coast Carbon cruises 1 & 2, and the Gulf of Mexico Ecosystem and Carbon Cycle cruise (Peng & Langdon, 2007; Wanninkhof et al., 2012; Barbero et al., 2017). Some regional datasets encompassing spatial and depth subsets do exist from individual research studies but mostly in relatively shallow coastal waters (Hu et al., 2018; Cai et al., 2011; Cai et al., 2020; Huang et al., 2015). The current state-of-the-art analytical techniques can accurately quantify carbonate system parameters in the lab with excellent precision (±0.2-0.4 $\mu mol \cdot kg^{-1}$ for total dissolved inorganic carbon or DIC and total titration alkalinity or TA, and ±0.0004 for pH) (Fajar et al., 2015; Douglas & Byrne, 2017). However, the ability to make direct carbonate system measurements in situ is restricted to select variables. For example, five (pCO_2, pH, DIC, TA,

CO_3^{2-}) out of the six (which also include HCO_3^-) carbonate system variables can be directly measured in lab. Although of these five parameters, only pH and pCO_2 have reached accessible autonomous measurements while autonomous TA and DIC measurements remain largely in experimental stages (Bresnahan et al., 2014; Takeshita et al., 2018; Seelmann et al., 2019; Byrne et al., 2011). However, pH and pCO_2 as the input variables for speciation calculations typically produce large errors (Orr et al., 2018). Regardless, directly measured carbonate system parameters are constrained across time and space, and this constraint hinders our understanding of the state and evolution of carbonate chemistry in many areas. In recent years, statistical modeling based on hydrographic data has been proposed as a viable and convenient alternative to fill in data gaps (Juranek et al., 2009), as such data (including salinity, temperature, DO) are much more widely available compared to the carbonate chemistry data (Table 1).

By creating models using commonly measured hydrographic data, information such as Ω_{Arag} and pH can be calculated or estimated for both the current and potentially historical times. This was first done for Ω_{Arag} on the continental shelf of central Oregon (Juranek et al., 2009), where a multilinear regression (MLR) model using temperature and oxygen was developed to estimate Ω_{Arag} with excellent fit ($R^2 = 0.987$, with relative mean standard error or RMSE of 0.053). The model was used for construction of a comprehensive water-column Ω_{Arag} values and led to the application of models for Ω_{Arag} determination using historical datasets in other studies. A study on the Sea of Japan (East Sea) applied a similar model to a historical dataset lacking Ω_{Arag}. This resulted in a comprehensive set of Ω_{Arag} data from 1960 to 2000 (Kim et al., 2010). Similar models have been proven effective and accurate for the prediction of Ω_{Arag} using other hydrographic parameters (McGarry et al., 2021; Alin et al., 2012; Bostock et al., 2013).

This study created MLR models for pH and Ω_{Arag} in the NWGOM by fitting these parameters using measured values of temperature, depth, pressure, salinity, and dissolved oxygen. This study will also serve as a valuable baseline of data for future research in the NWGOM.

CHAPTER II. METHODS

II.1 Data source/study area

Historical data describing the carbonate chemistry system in the GOM begins with the first and second GOMECC cruises in 2007 and 2012 (Table 2). These studies covered both the northern GOM coast and the U.S. East Coast with three and two transects, respectively, in the GOM (GOMECC-1 and GOMECC-2) (Peng & Langdon, 2007; Barbero et al., 2017). The third GOMECC cruise in 2017 encompassed the entire GOM coast across 10 transects which extended in part to deep waters beyond the shelf. In addition to these expeditions, some regional datasets that include carbonate chemistry in the GOM encompassing spatial and depth subsets also exist for individual research studies but focus largely on the shelf and northern to northeastern GOM coast (Hu et al., 2017; Cai et al., 2011; Cai et al., 2020; Huang et al., 2015).

A substantial portion of data used for this study were collected from the Galveston transect in the NWGOM taken during the GOMECC cruises 1 and 3 in July of 2007 and 2017, respectively (Figure 1) (Peng & Langdon, 2007; Barbero et al., 2017). More focused samples were collected on board the *R/V* Pelican and the cruises took place in April 20-24 and August 10-15, 2021 (Figure 2), on a project called "Ocean Acidification at a Crossroad" (XR), which was funded by NOAA's Ocean Acidification Program. The combined data set includes 481 data points from 23 stations.

II.2 Sampling approach and analytical methods

Seawater sampling was done according to the best practices for carbonate chemistry (Dickson et al., 2007). Samples were taken from the Niskin bottles into 250-ml ground-neck borosilicate glass bottles. Preservation of samples for carbonate chemistry analyses was done by the addition of 100 μL of a saturated $HgCl_2$ solution. Glass stoppers with the aid of Apiezon®L

grease and rubber bands were used to seal the samples. The GOMECC samples were analyzed on board the ship, including DO, DIC, and TA; nutrient samples were analyzed at the Atlantic Oceanographic and Meteorological Laboratory (AOML). For the two cruises in 2021, only dissolved oxygen was analyzed on board the ship. All other samples were brought to the lab at Harte Research Institute, and analyzed for DIC, pH, and TA. Nutrient samples were analyzed at Geochemical and Environmental Research Group at Texas A&M University.

For the GOMECC samples, DO was determined using an automated oxygen titrator with amperometric end-point detection (Culberson and Huang 1987). DIC was determined using coulometry with gas calibrations and Certified Reference Material (CRM) stability checks to ensure proper performance (with precisions of ± 1.37 μmol/kg) (Johnson et al., 1985). For the XR samples collection, DO was determined using Winkler titration (Winkler, 1888). DIC was determined using infrared spectrometry on a DIC analyzer (Apollo SciTech Inc.) with CRM to ensure the proper performance (with precisions of ±0.1%) (Chen et al., 2015). For all cruises, TA was analyzed using open-cell Gran titration; and pH was analyzed using a spectrophotometric method with purified m-cresol purple (Gran, 1952; Liu et al., 2011).

II.3 Modeling approach

This study created reliable region specific MLR models for Ω_{Arag} and pH using some combination of predictor variables (temperature, salinity, DO, and depth/pressure) determined by known relationships. All calculations and modeling were done using the software R (Ver. 4.1.2) and MatLab (Ver. R2021b). First, carbonate speciation was calculated with TA and DIC as the input variables (GOMECC) or DIC and pH as the input variable (XR as TA analysis was not yet completed at the time) using the MatLab version CO2SYS software (van Heuven et al., 2011) with carbonate dissociation constants from Mehrbach et al. (1973) refit by Dickson and Millero

(1987), the dissociation constant of bisulfate reported in Dickson (1990), the total boron concentration provided in Uppström (1974), and aragonite solubility constant from Mucci (1983) were used. Differences in calculated pH and Ω_{Arag} values due to omission of nutrient parameters have previously been negligible in the NWGOM, nutrient input was not used in calculations of carbonate speciation in the XR samples (Hu et al., 2018).

Regression analysis was done using R following the steps below. First, the data were duplicated and modified into a set containing all depths and a set containing only depths greater than 20 m, below the summer mixed layer depth (Muller-Karger et al., 2015). Second, each set was duplicated and modified again into a set containing all stations and a set containing only stations along the Galveston line (west of -94.3W longitude line) (Figure 2). This resulted in a total of four different subsets of the data (Model 1 = 327 observations, all stations, and depths > 20, Model 2 = 392 observations, all stations, and all depths, Model 3 = 190 observations, Galveston stations, and depth >20, Model 4 = 232 observations, Galveston stations, and all depths) (Table 3) to train four different models for each Ω_{Arag} and pH.

All models were trained using the following procedure. Z-scores (standardized values) of all independent variables were used in place of non-standardized values (Quinn and Keough, 2002). To avoid including outliers due to error, calculation of standardized residuals was performed for each observation. Observations with standardized residuals with absolute values larger than 3 were examined and removed on a case-to-case basis. Three data points resulted in standardized residuals of >3 and those observations were removed for suspected sampling or analysis error. A full model was created composed of all potential variables (salinity, depth/pressure, DO, temperature). The MuMIn package (Ver 1.46.0) was used in R to preform two dredges, one to rank models by corrected Akaike Information Criterion (AICc) and another

to rank by predicted residual error sum of squares (PRESS) (Barton, 2022). The final models were selected by AICc, PRESS, interpretability, parsimony, and applicability from comparable models (within 2 AICc of one another) (Burnham and Anderson, 2004). Variables included in the top models were checked for problematic collinearity using Variance Inflation Factor (VIF). Models with any variable scoring VIF > 10 were discarded and replaced with the next best model following the same criteria. The selected models were examined further for any potential errors using spline models, Shapiro-Wilkes test for normality, and RMSE. In general, the model with the lowest RMSE and PRESS values are considered to be the best. Some models had issues with curvature which were remedied in part with the addition of square terms. The package *car* (Fox & Weisberg, 2019) was used to visualize, illustrate, and transform data throughout this process.

For model validation it is ideal to compare the accuracy of the created models on novel data or data removed from the original dataset before training the model (Quinn and Keough, 2002). Due to the limited amount of data available to this study, it was not realistic for this project to pursue either of these methods of validation. Instead, PRESS statistics was applied to the models as it provides similar quantification of the model's ability to predict new data as PRESS quantifies the difference between the observed (one datapoint (i) at a time) and predicted value by the model when fitted to all observations except i (Quinn and Keough, 2002).

CHAPTER III. RESULTS

III.1 Water Masses

The GOM is composed of water bodies originating outside of the GOM, including Caribbean Surface Water (CSW), Subtropical Underwater (SUW), and Tropical Atlantic Central Water (TACW), as well as riverine discharges mainly from the Mississippi-Atchafalaya River system. These bodies of water reside in the upper 300 m of the GOM and can be distinguished from Gulf Common Water (GCW) by T-S relationships, apparent oxygen utilization (AOU), nitrate, and DIC (Cervantes-Díaz et al., 2022). As seen in Figure 3 there was variation in the water masses seen over the 4 cruises. The CSW characterized by potential temperature (θ) >22 ˚C, salinity between 36.0-36.6, and potential density (σ_θ) values <25.3 kg·m^{-3} was encountered much more in 2017 than other years. Data from the 2017 cruise displayed a particularly clear signature with a grouping of measurements with σ_θ values <23 kg·m^{-3}, θ of >28 ˚C, and salinity around 36.5, which was not encountered in any other cruises. Data from July 2007 and August 2021 include some data points that are classified as CSW on the lower half of the salinity and temperature boundaries. In April of 2021, there was very minimal presence of the CSW with a group of measurements with salinity around 36.4 and θ around 25 ˚C. As expected, many data points from all cruise periods fell into what is classified as the GCW with θ from 18-22 ˚C, salinity between 36.3 and 38.8, and σ_θ values from 25.3-26.3 kg·m^{-3} as well as TACW with θ from 7.9-20 ˚C, salinity between 34.9 and 36.6, and σ_θ values from 26.2-27.2 kg·m^{-3}. The SUW was not encountered in any of the cruises in this study. An unclassified portion of water column seen in this dataset displays characteristics of low salinity, high temperature, and σ_θ values <23 kg·m^{-3}, likely due to mixing waters with nearby freshwater discharge. This signature was not

seen in April 2021 and seen only in 5 measurements in July 2017 but seen in greater quantity and extremes in July 2007 and August 2021.

III.2 MLR model statistics

When all potential variables (temperature, depth, salinity, pressure, dissolved oxygen) were placed in linear combination, VIF results for most variables were greater than 10 due to their natural collinearity. However, when any combination of two independent variables alone was made VIFs were all less than 10, apart from depth and pressure as these two parameters provide near synonymous information and were not used in combination in any model. The VIF information suggests that there is no coupling between any of the predictor variables examined in this study in the NWGOM. All linear combinations of hydrographic parameters in the models presented here resulted in VIFs less than 10. All predictors tested were selected for use in one or more models.

The models chosen to predict both Ω_{Arag} and pH included different combinations of the following parameters: depth, salinity, temperature, pressure, DO, and square terms (Table 3). The models for estimation of Ω_{Arag} were able to do so with adjusted R^2 values ≥ 0.98, RMSE values ≤ 0.14, and PRESS values ≤ 0.14. The models for estimation of pH were able to do so with adjusted R^2 values ≥ 0.93, RMSE values ≤ 0.02, and PRESS values ≤ 0.03. As seen in Figures 4-5, neither of the residuals for pH or Ω_{Arag} displayed depth-dependent bias. No clear pattern was seen in over- or underestimation relating to location in the water column by depth. Models for Ω_{Arag} were able to predict larger proportions of the variation than models predicting pH. However, RMSE and PRESS statistics indicate the models for pH displayed less deviation between predicted and actual values and may perform better when used with new data. These

model evaluative criteria indicate that both models produced reliable results across the range of observed values in the calibration dataset.

III.3 Spatial distributions of carbonate chemistry parameters (Ω_{Arag}, pH, DIC and TA)

Data collected in this study were used to construct depth contour plots for Ω_{Arag}, pH, DIC, and TA over the Galveston transect study area in July of 2007, July of 2017, April of 2021, and August of 2021 (Figures 6-9). Data were also used to create depth profiles for DO over the same time periods (Figure 10). These data plots allow for visualization of the spatial and temporal variation that occurred during this study.

All shelf and upper slope waters sampled were supersaturated ($\Omega_{Arag} > 1$) with highest values of 4.39 and lowest values of 1.03 (Figure 6). The depth profiles reconstructed for July 2007 show the $\Omega_{Arag} = 2.0$ isopleth at ~200 m, the $\Omega_{Arag} = 1.5$ isopleth at ~350 m, and a portion of the water column at or below the $\Omega_{Arag} = 1.1$ isopleth at 600 m. The depth profiles for July 2017 show the $\Omega_{Arag} = 2$ isopleth at ~180 m, the Ω_{Arag}=1.5 isopleth at 330 m, and a portion of the water column at or below the $\Omega_{Arag} = 1.1$ isopleth at 550 m. The depth profiles reconstructed for April 2021 show the $\Omega_{Arag} = 2$ horizon at 200 m, the $\Omega_{Arag} = 1.5$ isopleth at 320 m, and a portion of the water column at or below the $\Omega_{Arag} = 1.1$ isopleth at 570 m. The depth profiles for August 2021 show the $\Omega_{Arag} = 2$ horizon at 180 m, the $\Omega_{Arag} = 1.5$ isopleth at 300 m, and a portion of the water column at or below the $\Omega_{Arag} = 1.1$ horizon at 570 m. The variation in Ω_{Arag} experienced over the shelf (less than 100 m) over the four cruises remained relatively consistent (±0.05). In all depth profiles the locations of the $\Omega_{Arag} = 1.5$ and $\Omega_{Arag} = 1.1$ isopleths coincide very closely with the upper and lower boundaries of the portion of the water column displaying DO values ≤ 125 µmol kg^{-1}. The $\Omega_{Arag} = 2$ and $\Omega_{Arag} = 1.1$ horizons varied ±20 and ±50 m, respectively. The $\Omega_{Arag} = 1.5$ isopleth decreased 50 m over the course of the study period consistently.

Depth distribution for pH revealed consistent spatial patterns over all four cruises although with different values (Figure 7). Profiles displayed similar maximum values over the entire shelf and upper 125 m and minimum values around depths of 500 m. In 2007, pH values fell below 8.0 at around 125 m, in 2021 this occurred at depths around 115 m. pH values fell below 7.9 at around 265±5 m consistently from all cruises. Maximum values of pH over the shelf in July of 2007 reached 8.139 while in April and August of 2021 the maximum pH values were 8.099 and 8.108, respectively, between 0.031-0.050 units lower. Minimum pH values experienced over the shelf also varied from 7.828 in 2007 to 7.813 and 7.816 in April and August 2021 for a decrease of 0.012-0.015 units. The ranges of pH experienced over the shelf in 2007 and 2021 were 0.311 and 0.289 (when April and August 2021 values were averaged). Temporal variation from 2007 to 2021 shows a variation of the pH = 8.0 isopleth by 10 m while the pH = 7.9 isopleth remained at similar depth. Larger variations were noted over the shelf where a 0.022 units smaller range of pH values was experienced with lower maximums by 0.036 and lower minimums by 0.013 (when April and August 2021 values were averaged).

Depth profiles for DO exhibit a consistent relationship with depth over all study periods, with high values at the surface layer, DO minimums around 400 m and gradual increase with depth after (Figure 10). Spatial variation is visible, data collected at higher latitudes (closer to the coast) and in shallow waters (< 200 m) display larger variations than other regions. Additionally, data collected outside of the Galveston line to the east in the 2021 cruises display higher DO values. For data collected along the Galveston line, the oxygen minimum in 2007 was 112.7 $\mu mol\ kg^{-1}$ at 355 m and DO was below 115.0 $\mu mol\ kg^{-1}$ from 347-405 m. In 2017 the oxygen minimum was 109.4 $\mu mol\ kg^{-1}$ at 398 m and DO was below 115 $\mu mol\ kg^{-1}$ from 248-516 m. In April 2021, the oxygen minimum was 109.5 $\mu mol\ kg^{-1}$ at 400 m and DO was below 115.0 µmol

kg^{-1} from 300-500 m. In August 2021, the oxygen minimum was 110.7 µmol kg^{-1} at 300 m and DO was below 115.0 µmol kg^{-1} from 300-400 m. Outside of the Galveston line, in April and August of 2021 oxygen minimums were 112.4 and 108.0 µmol kg^{-1} at 350 and 400 m. In April, no portion of the water column remained below 115 µmol kg^{-1}, however, in August DO values below 115 µmol kg^{-1} were seen from 300-500m. Over all cruises except August of 2021, the oxygen minimum remained consistently around 400 m. The upper boundary depth for DO at 115 µmol kg^{-1} has varied ~150 m mostly decreasing in depth over time. The thickness of the depth range at which the water column may experience low DO values (<115 µmol kg^{-1}) also varied temporally ~150 m. It is also important to note that the measured DO in the surface layer (<50 m) displayed large variation spatially in each dataset as well as temporally between cruises. This is important to consider in applicability of the models which contain DO as a variable for upper water column measurements.

CHAPTER IV. DISCUSSION

IV.1 Constraining data

One of the primary motivations behind the use of the simple MLR modeling with standardized variables to predict carbonate parameters is the ability to use the empirical relationships among predictor variables to accurately describe the controlling processes in the study area. Due to standardization the strength of the predictor variable can be inferred by the absolute value of the coefficient of variables included in the models (Quinn and Keough, 2002) (Table 3). In order to determine the most effective predictor variables of Ω_{Arag} and pH in the NWGOM, the data were quadruplicated and each copy was reduced to a different subset of the data to test for changes to the empirical relationships caused by depth or proximity to the Mississippi-Atchafalaya river outflow. The modifications of the four copies of data and the influence they are intended to test for are as follows: control dataset containing all data (model 1), dataset testing for influence of surface water containing depths > 20 m from all stations (model 2), dataset testing for combined effect of river proximity and surface water containing depths > 20 m and longitudes > 94.3 ˚W (limited to Galveston line stations) (model 3), dataset testing for effects of proximity to the river containing longitudes > 94.3 ˚W (model 4) (Table 3).

Removal of surface layer of water is regularly practiced in some capacity in carbonate modeling studies in order to eliminate variability due to influences beyond the scope of the model, such as surface water gas exchange, physical, biological and seasonal changes (McGarry et al., 2020; Juranek et al., 2009; Kim et al., 2010). In the NWGOM removal of shallow water can potentially mitigate the effects of the freshwater outflow as the low salinity river discharge is buoyant, although this is primarily addressed with the longitudinal restrictions. Depths to be removed explicitly for the purpose of removing the mixed layer vary from location and season of

study. Some models do not require exclusion of air-surface water interactions due to predictor variables being unaffected by this exchange and some have used removal of additional surface water as a means of removing the effect of seasonality (McGarry et al., 2021; Juranek et al., 2009; Kim et al., 2010; Muller-Karger et al., 2015). Due to the fact that all the models produced in this study contain DO, removing air-sea interaction was necessary. The removal of upper 50 meters to eliminate seasonality as done by Kim et al. (2010) would remove a substantial portion of the dataset in this study and thus is not viable here. Instead, 20 m removal was chosen as it is the depth of the mixed layer in summer in the GOM (Muller-Karger et al., 2015). Based on the final models chosen for Ω_{Arag} and pH, the relationships showed that the exclusion of the upper 20 m of the water column did slightly improve the performance of all models. When models for each parameter are compared with the model containing the same spatial data but all depths, models with the upper 20 m removed had either greater R^2, lower RMSE, lower PRESS, or a combination of the three (Table 3). The improvement seen in all models indicates that the removal of surface water does increase the applicability of the models. However, due to the small changes, more analysis with additional data including increased training data are needed to determine what degree of depth removal results in the most applicable model for the NWGOM.

The primary purpose of the constraints of longitude, limiting the eastern extent of the study area to the west of the 94.3 longitudinal line, is to test for and mitigate the effects of the freshwater outflow that can be transported westward over the Louisiana-Texas shelf (Morey et al., 2003). This narrower study area effectively eliminates the influence of the Mississippi Atchafalaya River System, as well as limits the study to the same stations repeatedly surveyed by all four cruises along the “Galveston Line” (Androulidakis et al., 2015). The performance of models with unrestricted data compared to those with longitude restrictions was variable. For

Ω_{Arag}, both models R^2, RMSE and PRESS improved or went unchanged when constrained (Table 3). For pH the exclusion of data from stations outside of the Galveston line increased R^2 values by 0.02 in both cases but left RMSE unchanged and increased the PRESS value of one model by 0.01. Due to the conflicting changes in performance of models with spatial restriction no conclusion can be made regarding existence of influence of eastern stations. As the changes in performance caused by the spatial restriction are relatively small and all models still perform well, the model is essentially equally applicable in the entire surveyed area, i.e., no exclusion of eastern stations.

IV.2 Drivers of carbonate system variability

IV.2.1 Aragonite saturation state

Due to the many controlling factors on Ω_{Arag} (K_{sp}, $[Ca^{2+}]$, $[CO_3^{2-}]$, DIC, and TA), temperature, salinity, pressure, and DO all have ties to Ω_{Arag} through interactions in carbonate chemistry and could be valuable in the prediction of Ω_{Arag}. Thus, the inclusion of temperature, pressure, and DO in the models is explained by known chemical relationships. Although predictors depth, salinity, and date were also tested, no model including these predictors was selected based on the criteria described in methods (Table 3).

Temperature was included in all models as the most important predictor of Ω_{Arag} variability in the NWGOM (Table 3). The strength of the relationship is chemically explained by Ω_{Arag} as a function of K_{sp} and $[CO_3^{2-}]$, and K_{sp} as a function of temperature, salinity, and pressure, and temperature also controls speciation of the carbonate system. The inclusion of temperature as a dominant predictor variable aligns well with models built for Ω_{Arag} prediction in other areas, which also found temperature to be the primary predictor of Ω_{Arag} variations (McGarry et al., 2021; Juranek et al., 2009; Alin et al., 2012; Kim et al., 2010; Bostock et al.,

2013) (Table 1). In the literature, it has been previously proposed that temperature is an important predictor of Ω_{Arag} in the upper 20 m of the oligotrophic waters of the NWGOM (Hu et al., 2018).

DO was included as the second most important predictor variable in all models (Table 3). The prominence of DO likely indicates the importance of the presence and variation of production and consumption of organic matter, for example, the DO minima appeared in the mid depth (~400 m) (Figure 3). A prior study also showed that biological activities are an influential factor in the study area (Hu et al., 2018).

IV.2.2 pH

Although anthropogenic CO_2 is the dominant driver of long□term change in pH in the open ocean, the variations observed in coastal waters on decadal time scales are largely attributed to driving forces including riverine input (carbon and nutrients) and ocean circulation changes (for example upwelling) (Feely et al., 2008; Cai et al., 2003; Yang et al., 2018; Salisbury et al., 2008; Duarte et al., 2013). The fact that DO was included in all pH models indicates the presence of biological activities as a driving force. DO was also found to be the strongest predictor of pH in the California current system and the Oregon shelf (Alin et al., 2012; McGarry et al., 2021) (Table 1).

Secondary and tertiary variables salinity and pressure (or depth) were included in models 1-3 but neither were included model 4, which only included DO and temperature, including their second order polynomial terms (Table 3). These shifts in variables may illustrate the influence that varying biological and physical processes due to the subset of the water column or longitudes have on pH. This influence is generated by the effect that these processes have on the

DO and DIC concentrations. (Alin et al., 2012). These empirical models show unique relationships between pH and DO and the additional influencing variables in the NWGOM.

IV.3 Comparisons with previous pH and Ω_{Arag} models

Although there are no existing models for the NWGOM, there are similar models that have been developed and applied in other areas. Due to the effects of differences in hydrography, river influences, and location on the drivers of the carbonate system, models are often specific to the geographic areas where they were created for. Although many of the primary drivers of the carbonate system remain the same, the secondary variables shift as does the degree to which they influence. Here I compare the accuracy and complexity of models created for other areas.

In the literature, Ω_{Arag} models have been created for the Northeast US (McGarry et al., 2021), Northern Gulf of Alaska (Evans et al., 2013), Central Oregon Coast (Juranek et al., 2009; Juranek et al., 2011), Southern California Current system (Alin et al., 2012), the Sea of Japan (East Sea) (Kim et al., 2010), and the Southern Ocean deep waters (Table 1) (Bostock et al., 2013). These models all have between 2 and 3 variables and adjusted $R^2 \geq 0.91$ in comparison to models produced here which have between 2 and 6 variables with an adjusted $R^2 \geq 0.93$. The primary predictor variable in all previous models except two (Evans et al., 2013; Juranek et al., 2011) is temperature, as is the case in this study. Most models also include some combination of temperature with salinity, oxygen, and interaction terms, and one model also used pressure (Kim et al., 2010), and one used NO_3^- (Evans et al., 2013). Models for the prediction of Ω_{Arag} are generally similar in the number and type of variables used. The models created in this study and those created previously for Ω_{Arag} agreed on the use of temperature in combination with DO as predictor variables.

pH models have been created for the northeast US (McGarry et al., 2021), the northeast pacific (Juranek et al., 2011), and the southern California current system (Table 1) (Alin et al., 2012). They included between 2 and 7 variables and resulted in adjusted $R^2 \geq 0.89$ in comparison to our models which have between 4 and 5 variables and adjusted $R^2 \geq 0.93$. All previous models agree with this study in that DO was the most important explanatory predictor variable used in the prediction of pH. Additionally, all models used temperature (McGarry et al., 2021; Alin et al., 2012; Juranek et al., 2011), one used an interaction term between DO and temperature (Alin et al., 2012), and one included nutrients, salinity and multiple interaction terms (McGarry et al., 2021). Although all models consistently depended on O_2 as the strongest predictor of pH variation and use temperature in some capacity, the choices for additional fitting parameters are diverse for these pH models.

IV.4 Data scarcity

Although the research and data collection regarding carbonate systems has increased in popularity and frequency, many areas especially the coastal ocean including the GOM are still undersampled and many datasets lack measurements to quantify carbonate chemistry needed for OA studies. Currently the coverage of data in the GOM is limited largely to public data from select transects and stations visited by research cruises such as GOMECC (Peng and Langdon, 2007; Barbero et al., 2017). New methods are being put into practice to remedy the missing data including autonomous measurements and modeling techniques like those used here.

New equipment has made autonomous measurements for selected variables via satellites, floats, and gliders possible. Although satellites provide large volumes of invaluable data, their scope is limited not only to the surface layer but only measurements of temperature and ocean color which can be interpreted for estimations of productivity, dissolved organic matter, and

carbonate chemistry parameters (Chen at al., 2019). Some remedies to the lack of data beyond the surface have come in the form of novel technologies including Argo floats and gliders. The Argo array presently supports more than 3000 floats supplying profiles of T and S, of which about 200 are also equipped with an O_2 sensor (Roemmich et al., 2019). Biogeochemical-Argo (BGC-Argo) floats can take measurements from surface to 2000 dbar and provide real time autonomous measurements for some combination of chlorophyll, particle backscatter, oxygen, nitrate, pH, or irradiance, with very few measuring all (Roemmich et al., 2019). Nevertheless, this equipment is limited in coverage ability and BGC-Argos have yet to reach the comprehensive coverage of traditional Argos. Gliders share the same biogeochemical sensors used by the BGC-Argos with similar mode of operations but perform saw-tooth trajectories surface to the bottom, or to 200–1,000 m depth limited largely by battery life and payload space hindering their ability to carry many sensors (Testor et al., 2019). Additionally, all data from floats and gliders must undergo rigorous quality control and correction of potential errors in sensors such as drift and compared to lab measured samples when possible (Roemmich et al., 2019). The need for full comprehensive accurate datasets will require the combination of all measurement techniques. In-situ sample collection and lab-based analyses are considered most accurate but lack realistic coverage, remote sensing and autonomous sensor data provide coverage ability but require much data validation for accuracy.

The capacity for autonomous observing of ocean carbonate chemistry is growing rapidly and by combining the real-time, high-resolution data with modeling methods it is possible to create comprehensive data coverage while simultaneously providing data validation via comparison between sources. With the use of MLR in combination with a single Argo profile float containing O_2 and temperature sensors, Juranek et al. (2011) was able to create a 14-month

comprehensive time series containing Ω_{Arag} and pH, which were verified by comparisons to novel data. Evans et al. (2013) applied models to novel data from glider flight and a GLOBEC mesoscale SeaSoar survey to create complete datasets, allowing for identification of variability of Ω_{Arag}. Although autonomous measurements have just begun, successful unison of models and autonomous data collection has been done and the increase of these endeavors should greatly improve geochemical data coverage and advance carbonate chemistry studies.

IV.5 Application of MLR

IV.5.1 Water masses

The importance of geographically localized MLR models is due to the differing hydrography of study areas and its effects on the predicted parameters. As seen in Figure 3, riverine discharge, and all water masses except for the Subtropical Underwater were encountered in this study. Based on the discussion in Alin et al. (2012), the models created in this study (the absence of a major water mass) may not account for potential changes in ocean circulation associated with warming. Large-scale shifts in coastal ocean circulation may affect the depth distribution of the water masses and their chemical signatures in the water depth zone that these empirical models cover. This reconstruction describes the water masses that have been included in the training of these models as well as serves as a baseline for the water mass composition in the NWGOM in the years 2007, 2017, and 2021. This baseline can be used in the future to observe potential shifts in circulation as well as to ensure models applicability to the inclusion of novel data.

IV.5.2 Temporal effect on MLR model fit

As concern about OA has grown, most carbonate system observations have been collected in recent years. The GOMECC-1 survey in 2007 was among the first to collect com-

prehensive measurements of inorganic carbonate system parameters in the GOM. Furthermore, there is motivation to apply the empirical models to future projections of ocean conditions to forecast the carbonate system conditions as OA progresses.

Previously created MLR have been applied to historical (40 year) and in-situ data (Juranek et al., 2011; Kim et al., 2010; Juranek et al., 2009; Evans et al., 2013). The temporal applicability of the model depends largely on timescale. Models can be used for prediction of past, and future data within approximately 10 years of the collection of the data used in its creation under assumptions that any seasonality or waterbody changes are captured by the model (Juranek et al. 2011). For example, Juranek et al. (2009) created a model using data collected only in spring and successfully used it to predict the seasonal changes in Ω_{Arag} under the assumption that the seasonal variability of the primary independent variables (temperature and DO) would be comparable to the variation encountered spatially during the initial data collection.

In order to use the model for predictions beyond the 10-year frame even with relatively unchanged circulation and watersheds, it is necessary to make corrections for shifts caused by changes in the anthropogenic CO_2 inventory in the water column. This is due to the fact that empirical models do not account for anthropogenic addition of CO_2, which changes the ratio of DIC/DO. After approximately 10 years the error due to anthropogenic emissions will exceed the model uncertainty (Juranek et al. 2011). Due to this, the models presented here should be accurate and applicable ±10 years, from approximately ~1997-2031. In order to extend the reconstruction further than 10 years it would first be necessary to account for the progressive addition (or subtraction) of anthropogenic CO_2 to the water column over time. For example, Kim et al. (2010) used estimates of anthropogenic CO_2 invasion to subtract anthropogenic CO_2 and

apply modeling estimates of DIC in the Sea of Japan (East Sea) to create a 40-year reconstruction.

In addition to long-term changes, there is strong motivation to apply the empirical models to year-round basic hydrographic data to reconstruct the seasonal cycle of carbonate chemistry. However, this model along with most other models were calibrated using mostly summer data (Davis et al., 2018). One method to avoid the problem of seasonal variations in the relationships between physical and chemical data is by excluding waters from depths influenced by local meteorological conditions from the analysis (Kim et al. 2010). Although removal of portions of the data to omit meteorological affects was not possible, seasonal application may be viable in the produced models for pH as it was explained primarily by biologically driven changes. Seasonal application may still be possible for Ω_{Arag} at depths 30–300 m as biological changes are primarily driven by DIC rather than TA (Hu et al., 2018; Anglès et al., 2019). It is expected that changes in DIC should be captured in these models due to their relationship with DO. This is because DIC and DO changes are expected to be proportional in remineralization zones (Hales et al., 2005; Anderson and Sarmiento, 1994). It has been previously observed that the seasonal variations in Ω_{Arag} in the GOM are influenced primarily by changes in temperature (Hu et al., 2018). As a result, it is possible that as the models developed here may still be able to predict seasonal variations of Ω_{Arag} reasonably well.

IV.5.3 Recommendation

Potential issues seen in all models indicate that the models, despite their strength, could be improved further. Shapiro–Wilk test, a test for normality, p-values <0.01 indicate non-normality in the residuals, this could be due to the large variation in the included shallow and mixed layers, need for more data points, or application of a more complex model. Future work to

improve these models includes additional data and potential application of non-linear or artificial intelligence (AI) models such as neural networks and locally interpolated regressions like those used by Carter et al. (2021). Data from GOMECC-4 in September 2021 are still in the processing stage at the time of this writing but on completion will be included in these models.

IV.6 Shoaling, upwelling and benthic Fauna

Although it is still largely unclear how organisms in the NWGOM could be affected by OA, laboratory experiments have indicated potentially deleterious impacts to organisms exposed to waters with low or decreased Ω_{Arag} (Kleypas et al., 2006; Fabry et al.,2008; Doney et al., 2009). Most lab experiments largely manipulate pCO_2 and pH conditions predicted for the open ocean in year 2100. However, coastal biogeochemical dynamics are governed by interactions between processes on land, in the open ocean, and the atmosphere, and the behavior may be different from the open ocean (Aufdenkampe et al., 2011). Upwelling in coastal areas combined with potential shoaling of Ω_{Arag} adds additional uncertainty and threat to benthic fauna in the coastal ocean. Included in the study area, is the Flower Garden Banks National Marine Sanctuary to the south of the Texas and Louisiana border, with a variety of habitats ranging in depth from 17-140m (Johnston et al., 2016). The depth profiles reconstructed with these data show that the depth of $\Omega_{Arag} = 2$ is located at ~180 m as of August 2021 but varied between 175-200 m between 2017 and 2021 (Figure 9). As the relatively low $\Omega_{Arag} = 2$ in the reconstructed data sits at 180-200 m, upwelling or substantial mixing could bring this water in contact with deep water corals and calcifiers of the Gulf residing at depths of up to 150 m (Gil-Agudelo et al., 2020). Although the depth of $\Omega_{Arag} = 2$ showed little variability from the four cruises, the seasonal upwelling of the low Ω_{Arag} waters is a documented occurrence in the NWGOM (Zavala-Hidalgo et al., 2006) and the upwelling intensity is likely to increase under future warming climate

scenarios with additional uptake of anthropogenic CO_2 (Bakun, 1990; Snyder et al., 2003). Furthermore, additional CO_2 will continue to decrease coastal Ω_{Arag} well into this century (Feely et al., 2008a). If climate impacts occur as predicted, upwelling and shoaling low Ω_{Arag} waters will bring the latter into coastal areas habited by calcifying organisms.

CHAPTER V. CONCLUSION

This study created models for the estimation of pH in the NWGOM that preformed reliably with $R^2>0.93$ and RMSE<0.03 (Table 1). The empirical relationships created illustrated DO as the dominant driver of pH variability. Depth profiles for pH revealed consistent contour patterns over all four cruises with highest values over the shelf and upper 125 m and minimum values around depths of 500 m (Figure 7). The pH = 7.9 isopleth remained around 270 m in all years and the pH = 8 isopleth remained around 120 m in all years. Over the shelf there was a lower maxima by 0.0356 and lower minima by 0.0133 creating a 0.0223 unit narrower range of pH values (April and August 2021 averaged).

The Ω_{Arag} models in the NWGOM have excellent performance with $R^2>0.98$ and RMSE<0.14 (Table 1). The empirical relationships demonstrate temperature and DO as the most important predictor variables. The data used to create the models were also used to create reconstructions that show variation of Ω_{Arag} over the timeframe of the study from 2007 to 2021 (Figure 6). The depth range of the water column between Ω_{Arag} = 2-1.5 decreased over the study period. The Ω_{Arag} = 2 and Ω_{Arag} = 1.1 varied 20 and 50 m, respectively, with movement in both directions while the Ω_{Arag} = 1.5 isopleth shoaled 50 m from 2007 to 2021. Relatively low Ω_{Arag} ($\Omega_{Arag} \leq 2$) was present in the 180 m depths. Mixing, upwelling, or further atmospheric CO_2 uptake could bring the low Ω_{Arag} waters into contact with benthic fauna of the Gulf. As more information on the impacts of decreased coastal Ω_{Arag} on coastal organism and temporal coverage of Ω_{Arag} into the future becomes available, the potential ramifications will be better understood.

Some caveats exist for the model application include seasonality, temporal gap from the creation to application of the model, and ocean circulation changes. First, all data collected for

this study occurred in the spring and summer months, therefore its accuracy in its application on an annual scale could be affected. Although some surface water data were removed, this removal may not be sufficient to account for all seasonal influence. The model for Ω_{Arag} includes temperature as a primary predictor which may allow the models to perform reliably in seasonal application. Further study should be done before applying the empirical models presented here outside of spring and summer months (Hales et al., 2005; Anderson and Sarmiento, 1994). Second, for application of these empirical models over time they must be adjusted on 10-year intervals to account for the additional anthropogenic CO_2 in seawater. Finally, changes in ocean circulation that bring in water masses that the model was not trained on will likely affect its accuracy. For this case, if the presence of SUW becomes significant or significant increase in river discharge were to occur in the sample area, model application should not be considered without further training.

The empirical model equations produced in this study using hydrographic and carbonate system parameters demonstrate their relationships in the NWGOM. Temperature was found to be the dominant driver of variability Ω_{Arag} and DO as the dominant driver of variability in pH. The data reconstructions done by this study have allowed for the identification of water masses regularly present in the NWGOM over the four sampling periods as well as portions of water column with low salinity, high temperature, and low density surface water influenced by riverine discharge. This study presents empirical models that contribute to the understanding of processes in the NWGOM and has begun a process of creating a complete and dynamic model to describe carbonate chemistry in this area. As more data become available, refined models as well as creation of additional models will improve our understanding of the spatial and temporal variations experienced in the physical and chemical parameters in this region.

Table 1 A comparison of previously published MLR models for Ω_{Arag} or pH.

Author	Geographic Area	Date	Variables	R^2 for Ω_{Arag}	Variables	R^2 for pH
Evans	Northern Gulf of Alaska	2013	S, NO_3	0.91	-	-
Bostock	South- ern Hemisphere	2013	T, S, O_2	0.99	-	-
Alin	Southern California Current System	2012	T, O_2, T·O_2	0.92	O_2, T, T*O_2	0.98
Kim	Sea of Japan (East Sea)	2010	T, P, O_2	0.995	-	-
Juranek	central Oregon	2009	T, T*O_2	0.987	-	-
Juranek	NE Pacific	2011	O_2, T, T*O_2	0.987	O_2, T	0.98
McGarry	Northeast US	2021	T, S	0.93	O_2, S, T, N, T*S, S*O_2, O_2*N	0.89

Table 2 Information of sampling cruises that collected data for this study.

Cruise ID	Date	Stations	Samples
R/V Pelican 1	April 20-24, 2021	23	155
R/V Pelican 2	August 10-15, 2021	23	173
GOMECC 1	July 2007	8	78
GOMECC 3	July 2017	8	75

Table 3 MLR models created in this study. Each parameter (Ω_{Arag} and pH) has four different models that used either the who dataset or subsets of these data.

	Predicting	Data	Coefficients	Variables	R^2	RMSE	PRESS
Model 1	Ω_{Arag}	Depths >20m All stations	0.733 0.3325 -0.0377	Temperature DO Temperrature^2	0.99	0.11	0.13
Model 2	Ω_{Arag}	All depths All stations	0.6572 0.356 -0.1338 -0.0312	Temperature DO Pressure DO^2	0.98	0.14	0.14
Model 3	Ω_{Arag}	Depths >20m Galveston line stations	0.7676 0.3451 -0.0547	Temperature DO Temperrature^2	0.99	0.09	0.1
Model 4	Ω_{Arag}	All depths Galveston line stations	0.6684 0.371 -0.1649 -0.0486	Temperature DO Pressure DO^2	0.99	0.12	0.14
Model 1	pH	Depths >20m All stations	0.063 -0.0219 0.021 -0.01	DO Pressure Salinity DO^2	0.94	0.02	0.02
Model 2	pH	All depths All stations	0.0605 -0.029 0.0201 -0.0112 0.0055	DO Depth Salinity DO^2 Salinity^2	0.93	0.02	0.03
Model 3	pH	Depths >20m Galveston line stations	0.0636 0.0235 -0.0209 -0.0104	DO Salinity Depth DO2	0.96	0.02	0.03
Model 4	pH	All depths Galveston line stations	0.0674 -0.0333 0.0186 -0.0132	DO Temperrature^2 Temperature DO^2	0.95	0.02	0.03

Figure 1 Locations of the sampling stations during the GOMECC cruises. Red square highlights the subset of stations used in this study.

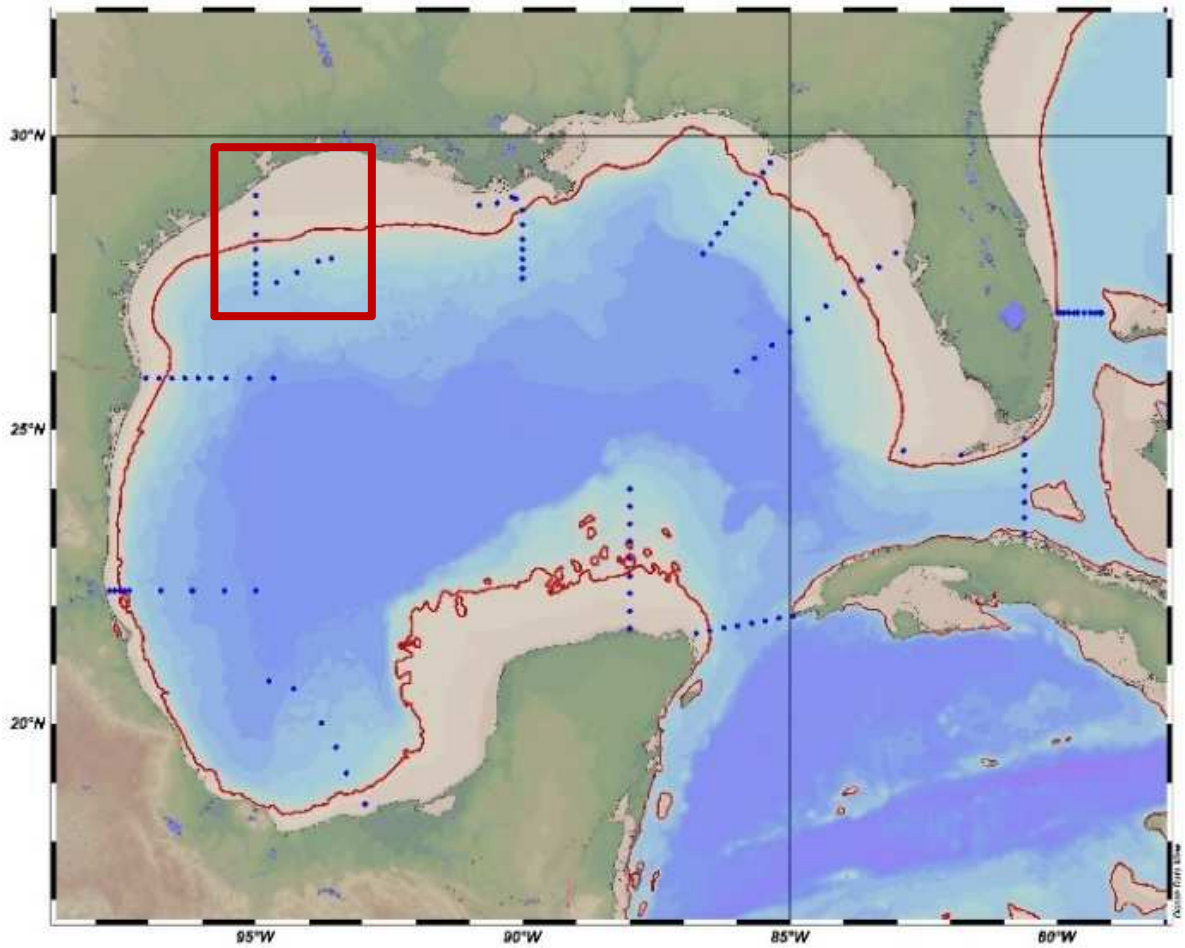

Figure 2 Sampling locations during the Ocean Acidification at a Crossroad (XR) cruises. Black filled points illustrate the stations used in the "Galveston Line" data subsets .

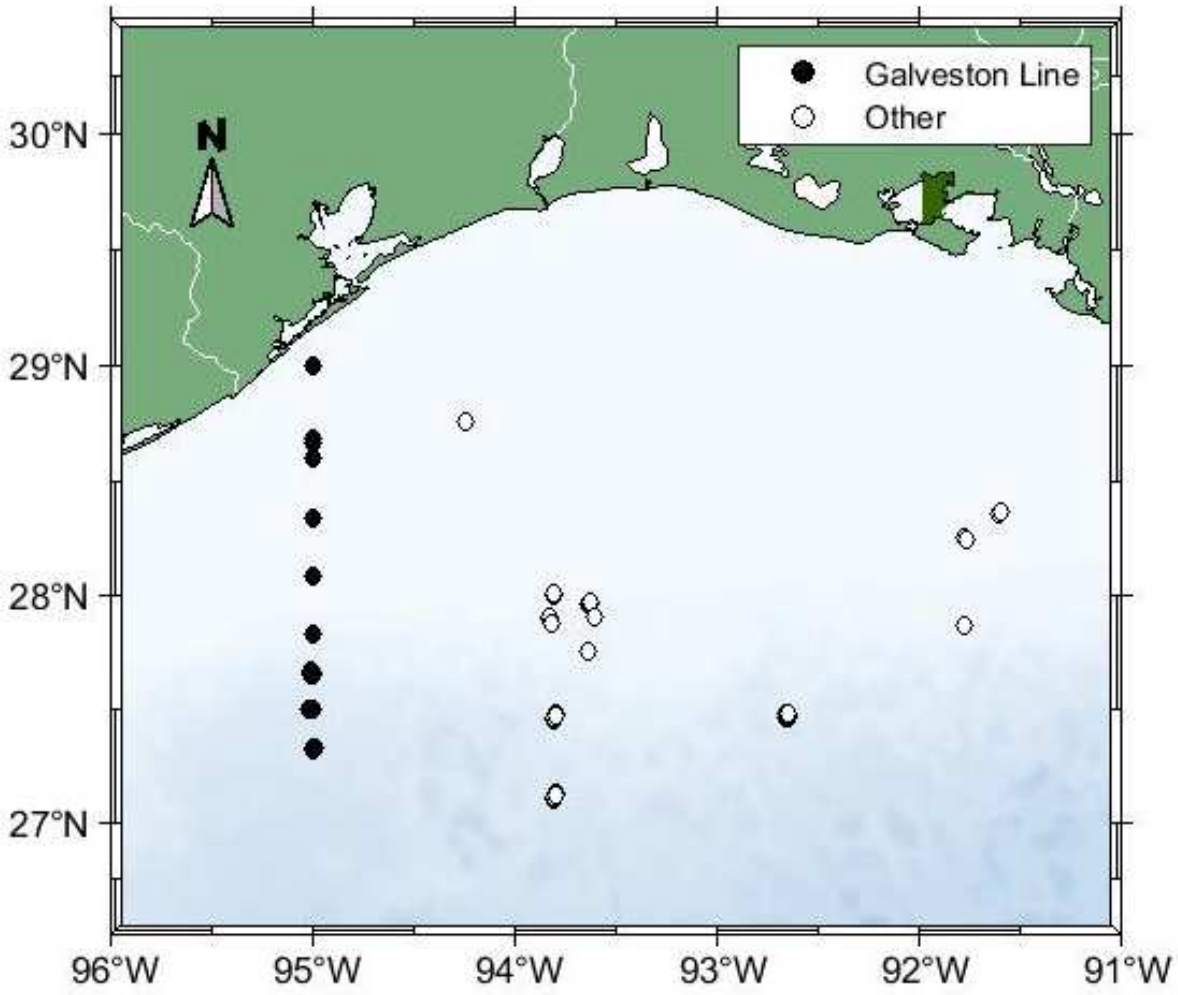

Figure 3 A scatter plot of all collected data as explained by potential temperature and salinity. The green contour lines represent potential density (Variable description and units: temperature, potential temperature ˚C; Salinity, practical salinity; potential density, kg·m^{-3}).

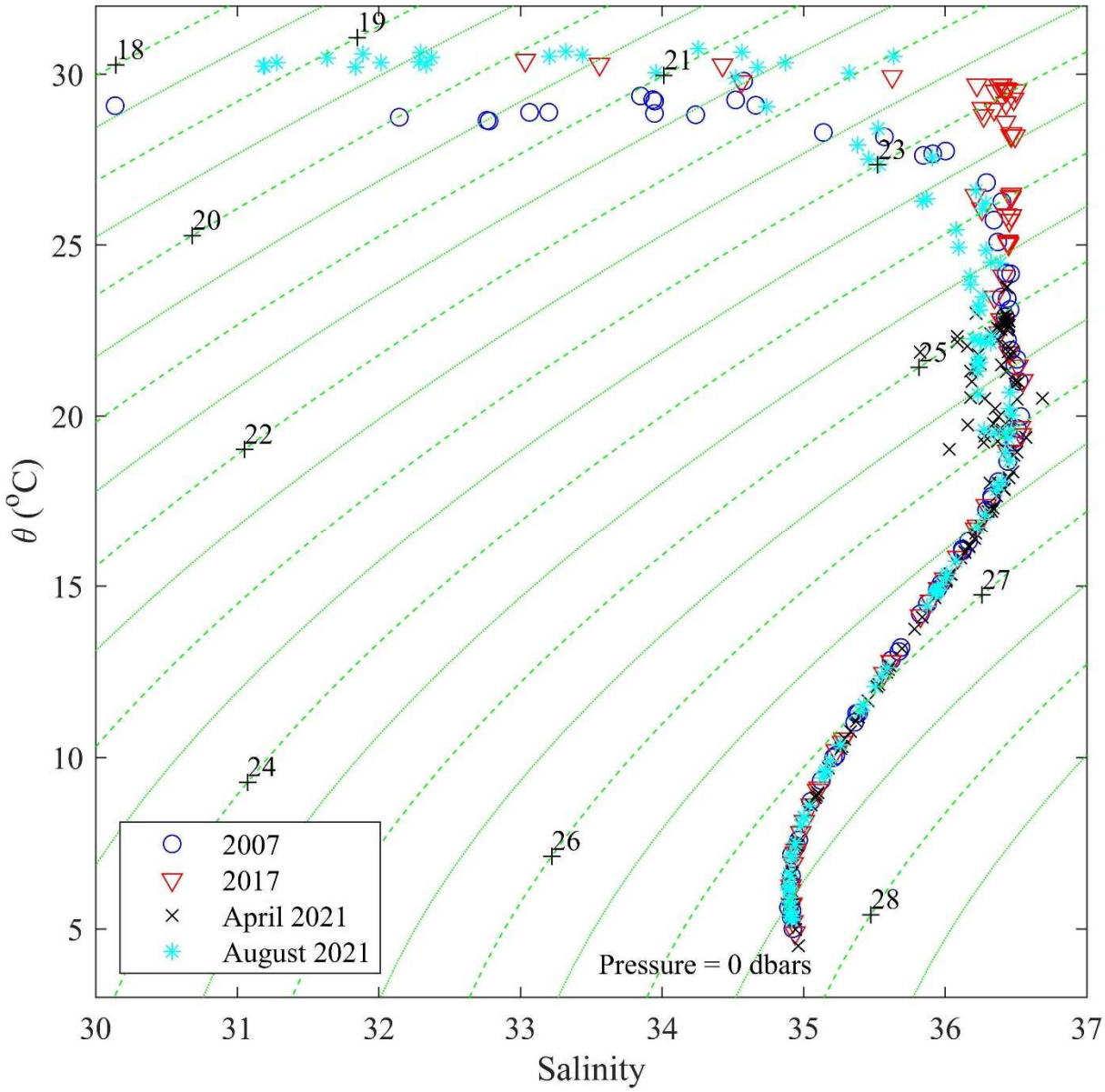

Figure 4 | Boxplots illustrating the distribution of residuals from all pH models. Depths indicate groupings of observations from 50 m intervals of the water column (i.e., Boxplot marked 100 included residuals from predictions using measurements collected from 50-100 m).

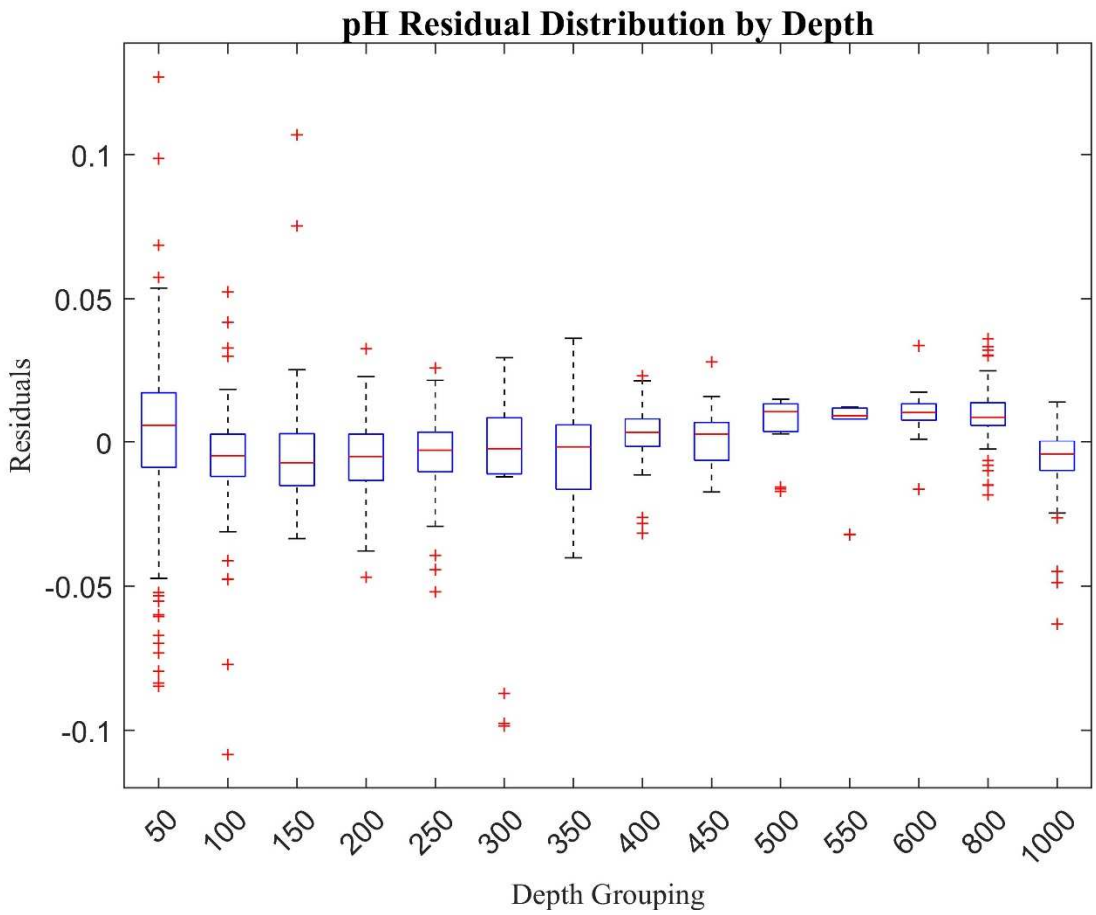

Figure 5 Boxplots illustrating the distribution of residuals from all Ω_{Arag} models. Depths indicate groupings of observations from 50 m intervals of the water column (i.e., Boxplot marked 100 included residuals from predictions using measurements collected from 50-100 m).

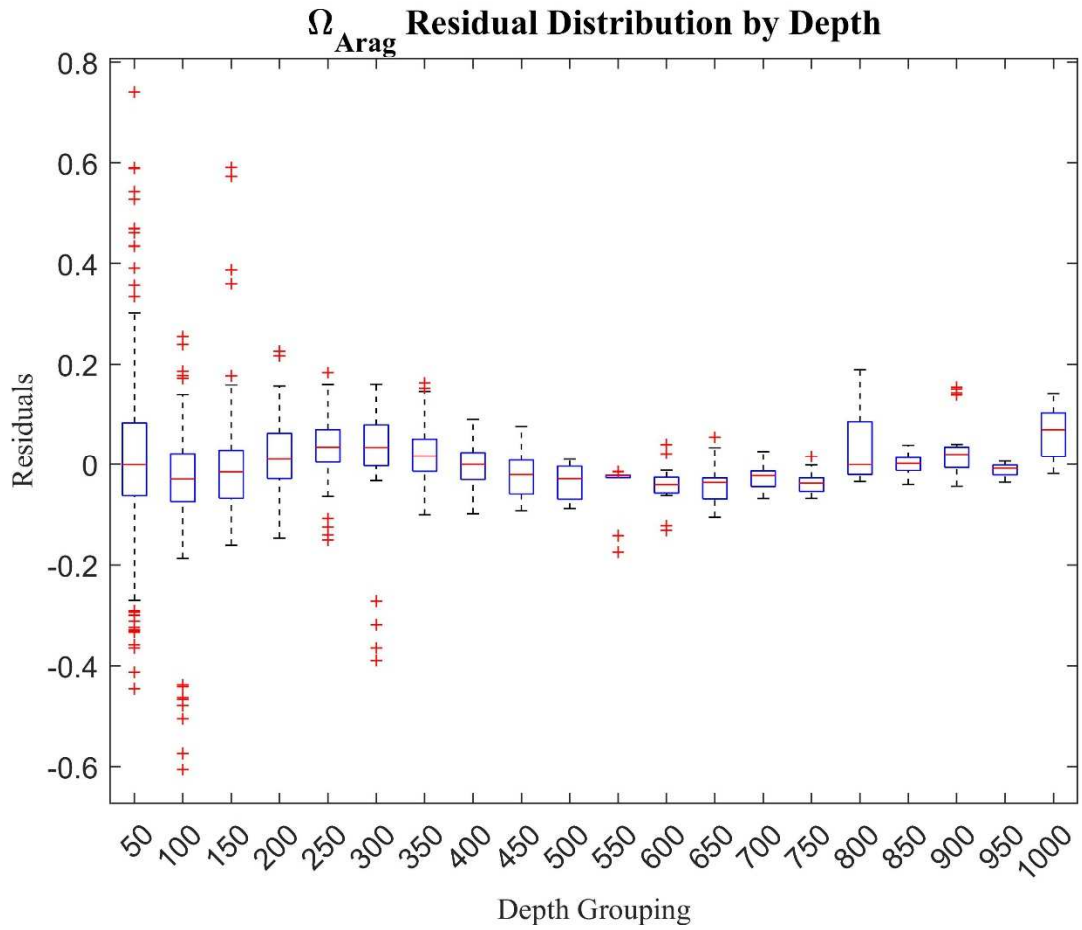

Figure 6 Contour plots showing the distribution of Ω_{Arag} over the Galveston line stations. The solid line represents $\Omega = 2$. The dashed line represents $\Omega = 1.5$. The dotted line represents $\Omega = 1.1$ (Variable description and units: Depth, m).

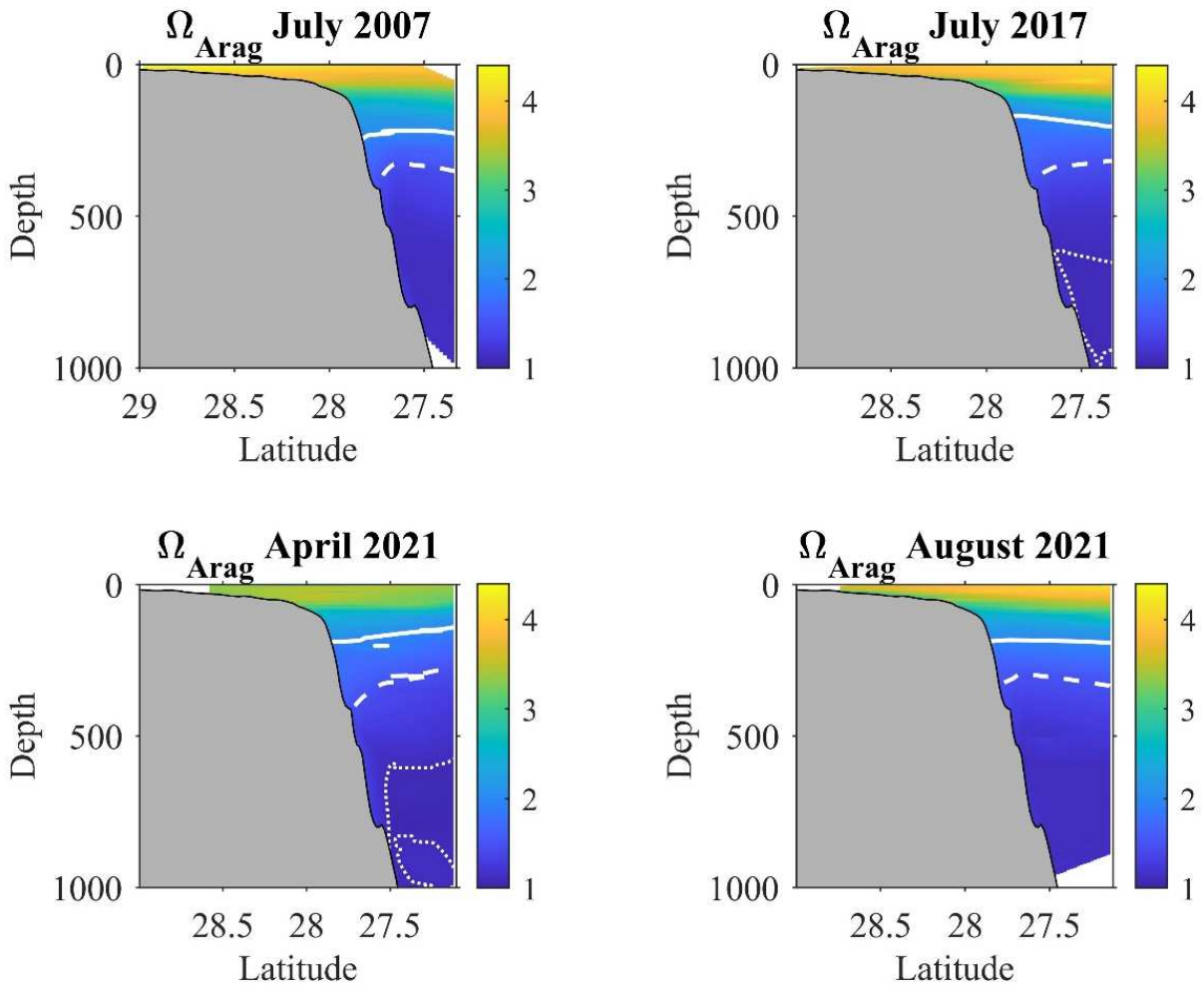

Figure 7 Contour plots showing the distribution of pH over the Galveston line stations. The dashed line represents pH = 8. The dotted line represents pH = 7.9 (Variable description and units: Depth, m).

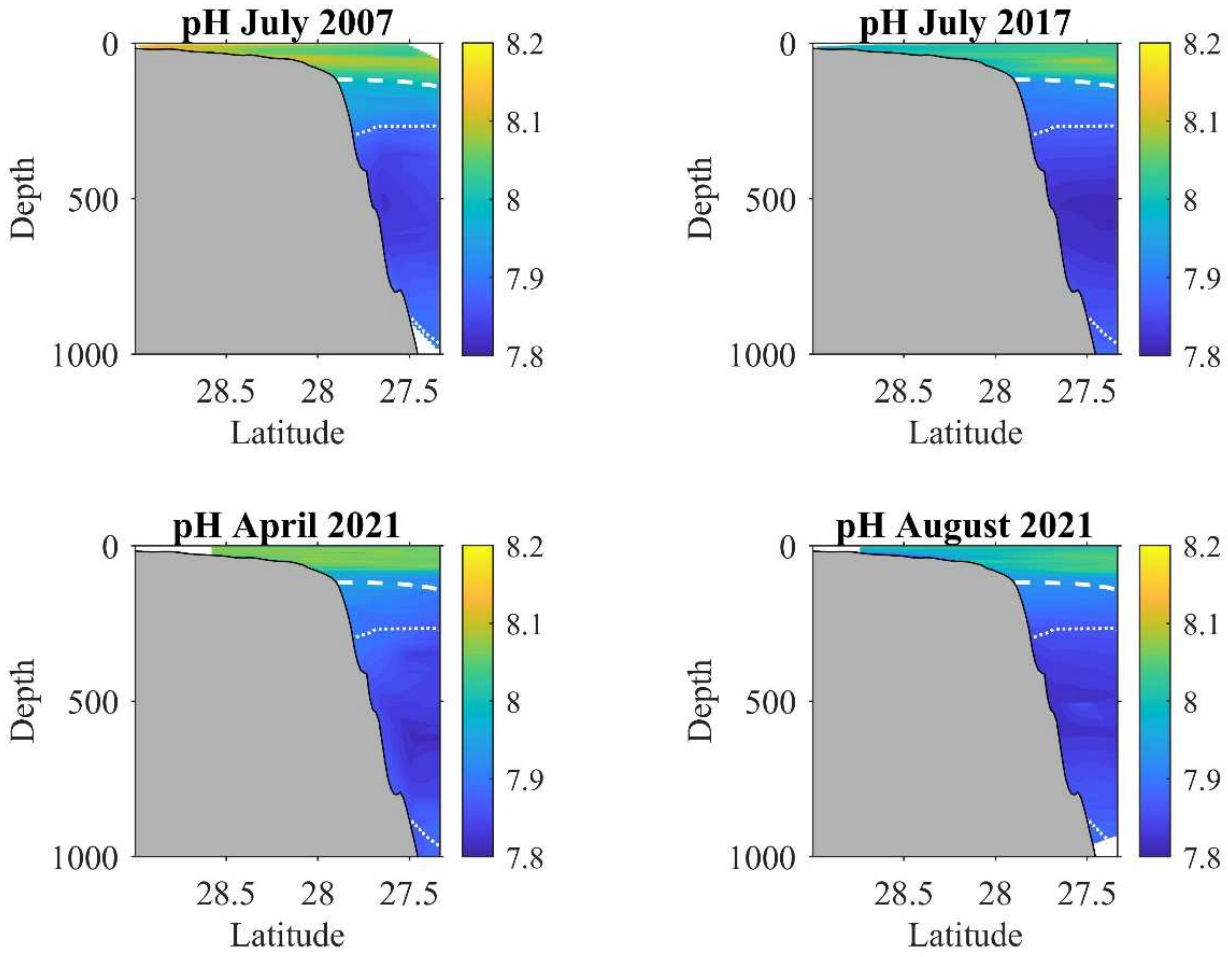

Figure 8 Contour plots showing the distribution of DIC over the Galveston line stations (Variable description and units: Depth, m; DIC, μmol kg^{-1}).

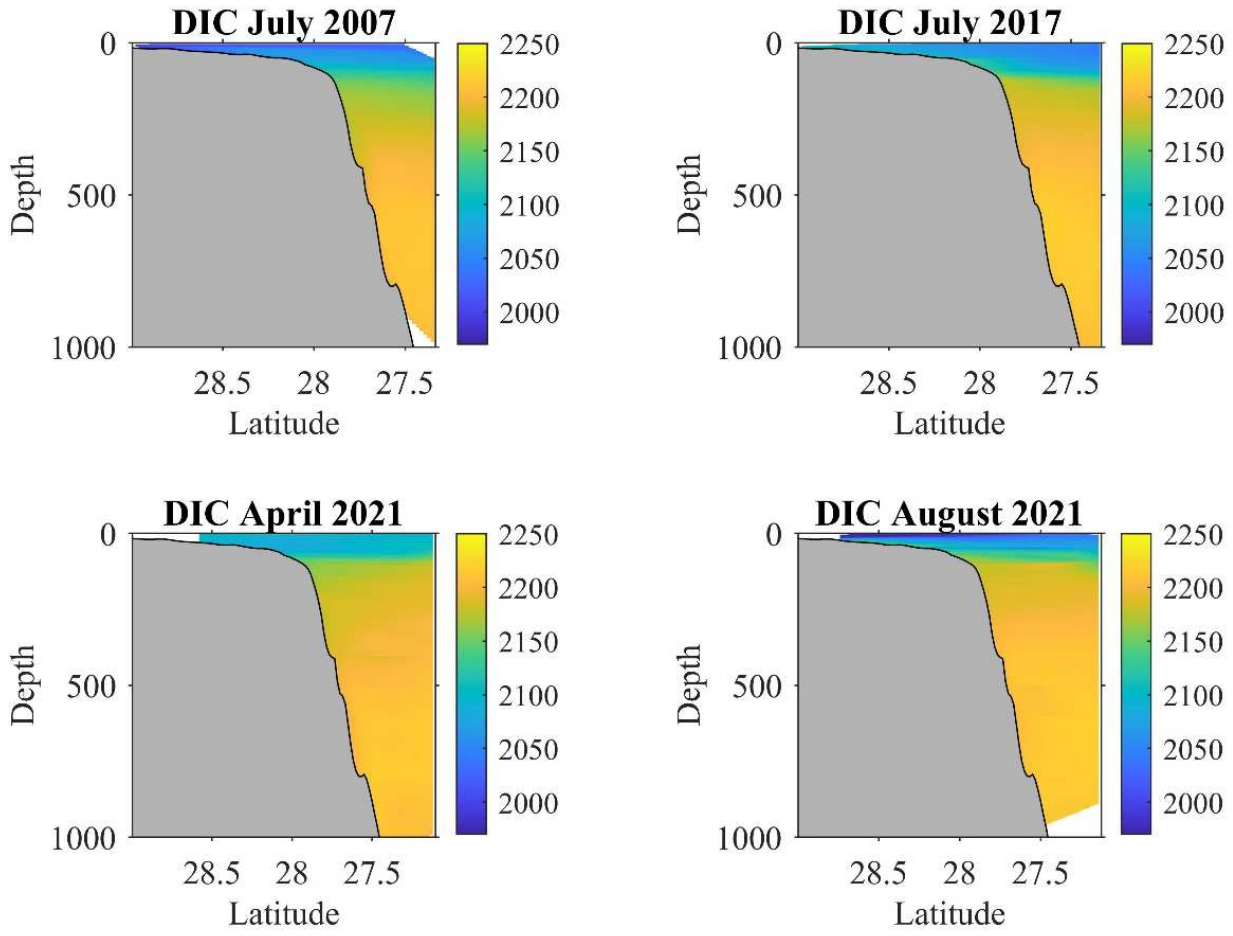

Figure 9 Contour plots showing the distribution of TA over the Galveston line stations (Variable description and units: Depth, m; TA, μmol kg^{-1}).

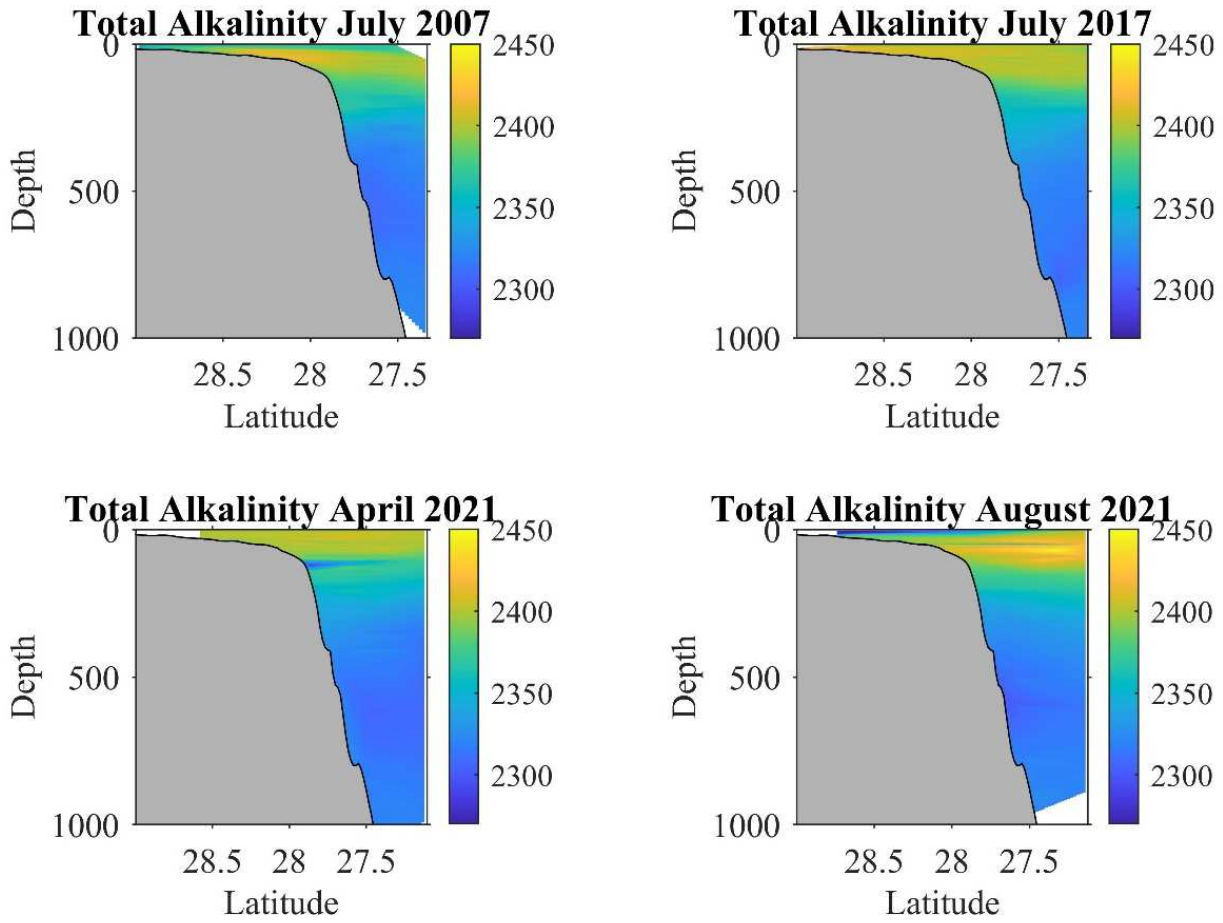

Figure 10 Depth profiles of DO concentration using collected data from all stations. The color filling shows latitude of each data point (Variable description and units: DO, μmol kg^{-1}; Depth, m).

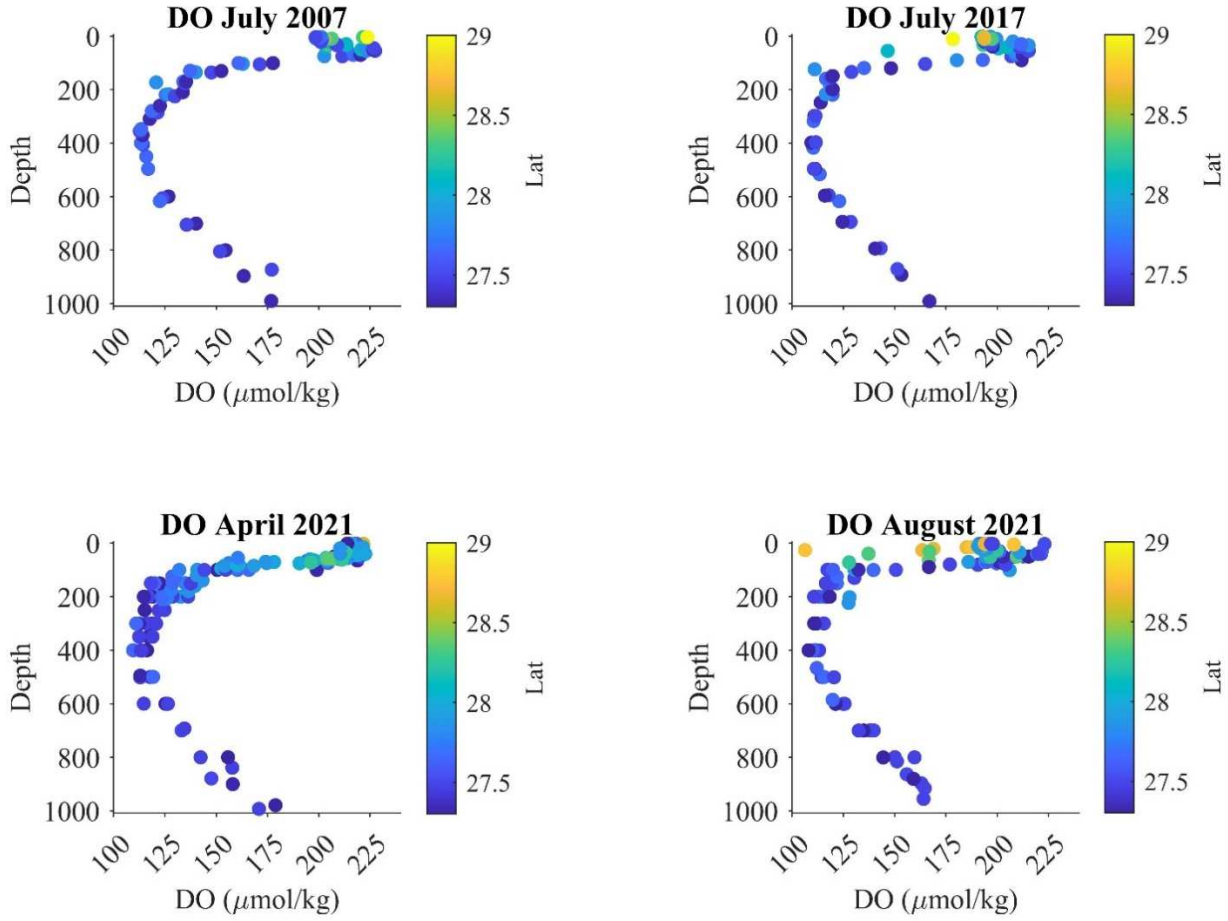

Figure 11 Predicted versus measured values in Ω_{Arag} models based on the entire dataset or different subsets (see Table 3 for details).

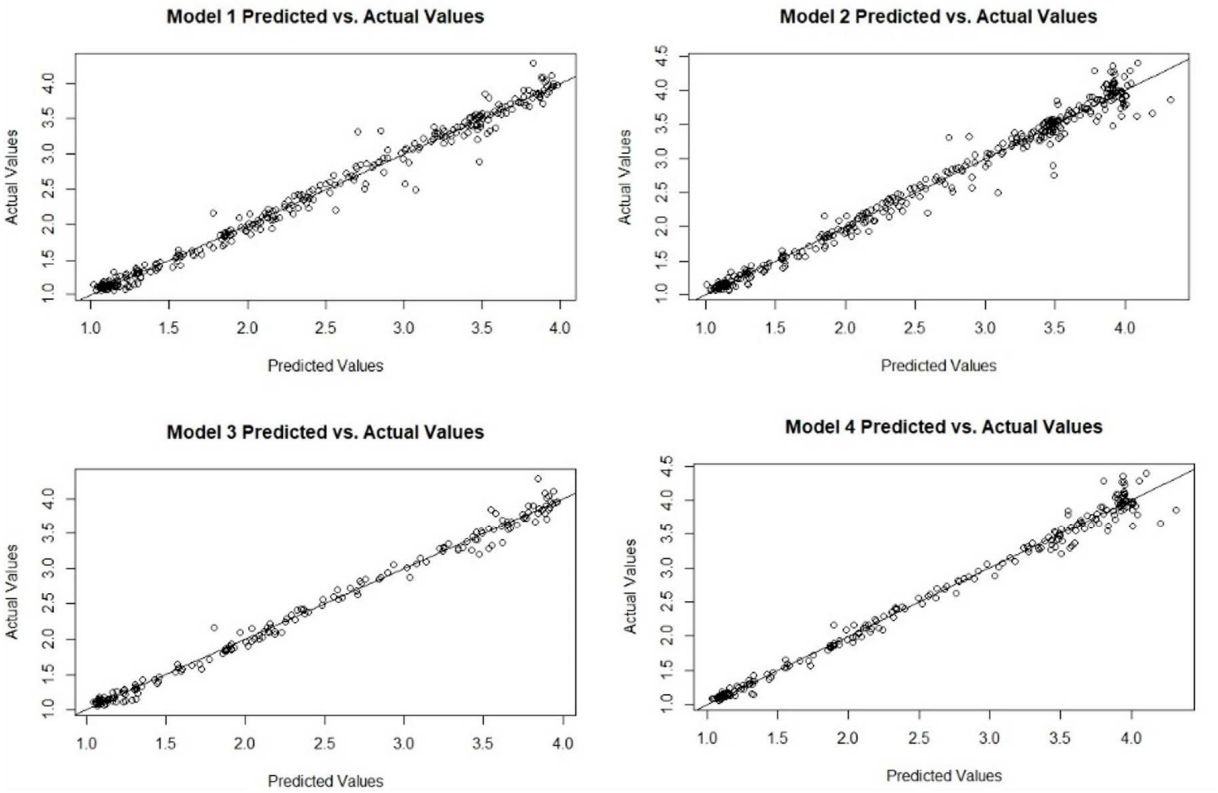

Figure 12 Predicted versus measured values in pH models based on the entire dataset or different subsets (see Table 3 for details).

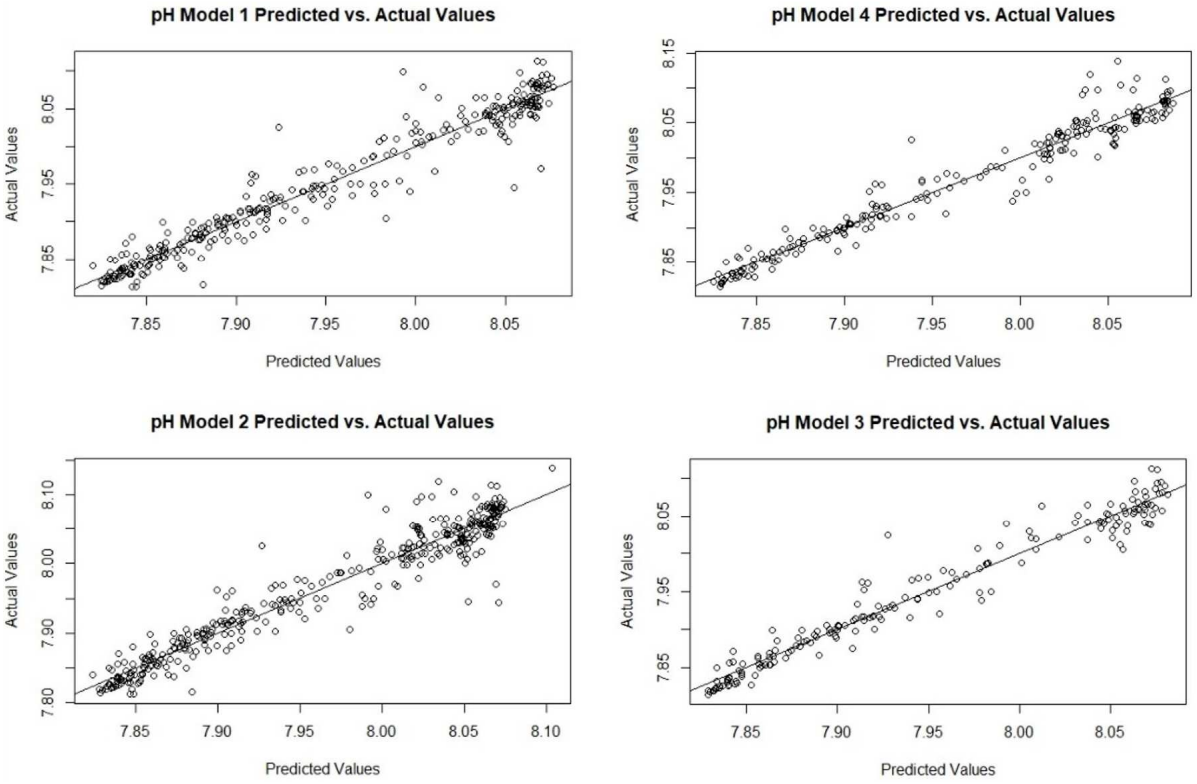

LITERATURE CITED

Anderson, L. A., & Sarmiento, J. L. (1994). Redfield ratios of remineralization determined by nutrient data analysis. *Global Biogeochemical Cycles*, *8*(1), 65–80. https://doi.org/10.1029/93GB03318

Albright, R., Takeshita, Y., Koweek, D. A., Ninokawa, A., Wolfe, K., Rivlin, T., Nebuchina, Y., Young, J., & Caldeira, K. (2018). Carbon dioxide addition to coral reef waters suppresses net community calcification. *Nature 555*(7697), 516–519. https://doi.org/10.1038/nature25968.

Alin, S. R., Feely, R. A., Dickson, A. G., Martín Hernández-Ayón, J., Juranek, L. W., Ohman, M. D., & Goericke, R. (2012). Robust empirical relationships for estimating the carbonate system in the southern California Current System and application to CalCOFI hydrographic cruise data (2005–2011). *Journal of Geophysical Research: Oceans, 117*(C5), 5033. https://doi.org/10.1029/2011JC007511

Androulidakis, Y. S., Kourafalou, V. H., & Schiller, R. V. (2015). Process studies on the evolution of the Mississippi River plume: Impact of topography, wind and discharge conditions. *Continental Shelf Research*, *107*, 33–49. https://doi.org/10.1016/j.csr.2015.07.014

Anglès, S., Jordi, A., Henrichs, D. W., & Campbell, L. (2019). Influence of coastal upwelling and river discharge on the phytoplankton community composition in the northwestern Gulf of Mexico. *Progress in Oceanography, 173*, 26–36. https://doi.org/10.1016/J.POCEAN.2019.02.001

Anthony, K. R. N., Kline, D. I., Diaz-Pulido, G., Dove, S., & Hoegh-Guldberg, O. (2008). Ocean acidification causes bleaching and productivity loss in coral reef builders. *Proceedings of*

the National Academy of Sciences, *105*(45), 17442–17446. https://doi.org/10.1073/PNAS.0804478105

Aufdenkampe, A. K., Mayorga, E., Raymond, P. A., Melack, J. M., Doney, S. C., Alin, S. R., Aalto, R. E., & Yoo, K. (2011). Riverine coupling of biogeochemical cycles between land, oceans, and atmosphere. *Frontiers in Ecology and the Environment, 9*(1), 53–60. https://doi.org/10.1890/100014

Bakun, A. (1990). Global climate change and intensification of coastal ocean upwelling. *Science*, *247*(4939), 198–201. https://doi.org/10.1126/science.247.4939.198

Barbero, L., Pierrot, D., Wanninkhof, R., Baringer, M., Hooper, J., Zhang, J. Z., Smith, R., Byrne, R., Langdon, C., Hernández-Ayón, M., Schnetzer, A., Stauffer, B., Herzka, S., Cano-Compairé, J., Hernández, F., Pech, D., Hu, C., English, D., Ondrusek, M., … Derr, G. (2017). *Cruise Report: Third Gulf of Mexico Ecosystems and Carbon Cycle (GOMECC-3) Cruise*. https://doi.org/10.25923/y6m9-fy08

Barton, Kamil. (2022). Multi-Model Inference (1.46.0).

Bayraktarov, E., Stewart-Sinclair, P. J., Brisbane, S., Boström-Einarsson, L., Saunders, M. I., Lovelock, C. E., Possingham, H. P., Mumby, P. J., & Wilson, K. A. (2019). Motivations, success, and cost of coral reef restoration. *Restoration Ecology*, 27(5), 981–991. https://doi.org/10.1111/REC.12977

Beck, M. W., Brumbaugh, R. D., Airoldi, L., Carranza, A., Coen, L. D., Crawford, C., Defeo, O., Edgar, G. J., Hancock, B., Kay, M. C., Lenihan, H. S., Luckenbach, M. W., Toropova, C. L., Zhang, G., & Guo, X. (2011). Oyster reefs at risk and recommendations for conservation, restoration, and management. *BioScience*, 61(2), 107–116. https://doi.org/10.1525/bio.2011.61.2.5

Bednaršek, N., Tarling, G. A., Bakker, D. C. E., Fielding, S., Jones, E. M., Venables, H. J., Ward, P., Kuzirian, A., Lézé, B., Feely, R. A., & Murphy, E. J. (2012). Extensive dissolution of live pteropods in the Southern Ocean. Nature Geoscience, 5(12), 881–885. https://doi.org/10.1038/NGEO1635

Bell, J. D., & Galzin, R. (1984). Influence of live coral cover on coral-reef fish communities. *Marine Ecology Progress Series*, 15, 265–274.

Bostock, H. C., Mikaloff Fletcher, S. E., & Williams, M. J. M. (2013). Estimating carbonate parameters from hydrographic data for the intermediate and deep waters of the Southern Hemisphere oceans. *Biogeosciences*, *10*(10), 6199–6213. https://doi.org/10.5194/BG-10-6199-2013

Bresnahan, P. J., Martz, T. R., Takeshita, Y., Johnson, K. S., & LaShomb, M. (2014). Best practices for autonomous measurement of seawater pH with the Honeywell Durafet. *Methods in Oceanography, 9*, 44–60. https://doi.org/10.1016/J.MIO.2014.08.003

Burnham, K. P., & Anderson, D. R. (2004). Multimodel Inference: Understanding AIC and BIC in Model Selection. Http://Dx.Doi.Org/10.1177/0049124104268644, 33(2), 261–304. https://doi.org/10.1177/0049124104268644

Byrne, R. H., Kaltenbacher, E., Steimle, E. T., & Liu, X. (2011). Design of autonomous in-situ spectrophotometric systems for measurement of nutrients and CO 2-system parameters. In K. Harada & T. Dickey (Eds.), *Proceedings of the International Workshop on Autonomous Measurements of Biogeochemical Parameters in the Ocean*.

Cai, W.-J., Hu, X., Huang, W.-J., Murrell, M. C., Lehrter, J. C., Lohrenz, S. E., Chou, W.-C., Zhai, W., Hollibaugh, J. T., Wang, Y., Zhao, P., Guo, X., Gundersen, K., Dai, M., & Gong,

G.-C. (2011). Acidification of subsurface coastal waters enhanced by eutrophication. Nature Geoscience, 4, 766–770. https://doi.org/10.1038/NGEO1297

Cai, W. J., Xu, Y. Y., Feely, R. A., Wanninkhof, R., Jönsson, B., Alin, S. R., Barbero, L., Cross, J. N., Azetsu-Scott, K., Fassbender, A. J., Carter, B. R., Jiang, L. Q., Pepin, P., Chen, B., Hussain, N., Reimer, J. J., Xue, L., Salisbury, J. E., Hernández-Ayón, J. M., … Gledhill, D. K. (2020). Controls on surface water carbonate chemistry along North American ocean margins. *Nature Communications*, 11(1), 1–13. https://doi.org/10.1038/s41467-020-16530-z

Cai, W. J., Wang, Z. A., & Wang, Y. (2003). The role of marsh-dominated heterotrophic continental margins in transport of CO2 between the atmosphere, the land-sea interface and the ocean. *Geophysical Research Letters, 30*(16). https://doi.org/10.1029/2003GL017633

Carter, B. R., Bittig, H. C., Fassbender, A. J., Sharp, J. D., Takeshita, Y., Xu, Y.-Y., Álvarez, M., Wanninkhof, R., Feely, R. A., & Barbero, L. (2021). New and updated global empirical seawater property estimation routines. *Limnology and Oceanography: Methods, 2021*. https://doi.org/10.1002/LOM3.10461

Chen, B., Cai, W. J., Chen, L. (2015). The marine carbonate system of the Arctic Ocean: Assessment of internal consistency and sampling considerations, summer 2010. *Marine Chemistry*, 174–188. https://doi.org/10.1016/J.MARCHEM.2015.09.007

Chen, S., Hu, C., Barnes, B. B., Wanninkhof, R., Cai, W.-J., Barbero, L., Pierrot, D., & Hu, C. (2019). A machine learning approach to estimate surface ocean pCO 2 from satellite measurements. *Remote Sensing of Environment*, *228*, 203–226. https://doi.org/10.1016/j.rse.2019.04.019

Chou, W. C., Gong, G. C., Cai, W. J., & Tseng, C. M. (2013). Seasonality of CO2 in coastal oceans altered by increasing anthropogenic nutrient delivery from large rivers: Evidence

from the Changjiang-East China Sea system. *Biogeosciences*, 10(6), 3889–3899. https://doi.org/10.5194/BG-10-3889-2013

Cervantes-Díaz, G. Y., Hernández-Ayón, J. M., Zirino, A., Herzka, S. Z., Camacho-Ibar, V., Norzagaray, O., Barbero, L., Montes, I., Sudre, J., & Delgado, J. A. (2022). Understanding upper water mass dynamics in the Gulf of Mexico by linking physical and biogeochemical features. *Journal of Marine Systems*, *225*, 103647. https://doi.org/10.1016/j.jmarsys.2021.103647

Clark, T. D., Raby, G. D., Roche, D. G., Binning, S. A., Speers-Roesch, B., Jutfelt, F., & Sundin, J. (2020). Ocean acidification does not impair the behaviour of coral reef fishes. Nature 2020 577:7790, 577(7790), 370–375. https://doi.org/10.1038/s41586-019-1903-y

Clayton, T.D.; & Byrne, R.H. (1993). Spectrophotometric seawater pH measurements: total hydrogen ion concentration scale calibration of m-cresol purple and at-sea results. *Deep Sea Research Part I: Oceanographic Research Papers, 40*(10), 2115–2129. Doi: 10.1016/0967-0637(93)90048-8

Cloern, J. E. (2001). Our evolving conceptual model of the coastal eutrophication problem. *Marine Ecology Progress Series*, 210, 223–253. https://doi.org/10.3354/MEPS210223

Comeau, S., Cornwall, C. E., DeCarlo, T. M., Doo, S. S., Carpenter, R. C., & McCulloch, M. T. (2019). Resistance to ocean acidification in coral reef taxa is not gained by acclimatization. *Nature Climate Change*, 9(6), 477–483. https://doi.org/10.1038/s41558-019-0486-9

Cooley, S. R., & Doney, S. C. (2009). Anticipating ocean acidification's economic consequences for commercial fisheries. *Environmental Research Letters*, 4(2), 024007. https://doi.org/10.1088/1748-9326/4/2/024007

Culberson CH, Huang S (1987) Automated amperometric oxygen titration. *Deep-Sea Res. 34*: 875–880

Davis, C. v., Hewett, K., Hill, T. M., Largier, J. L., Gaylord, B., & Jahncke, J. (2018). Reconstructing aragonite saturation state based on an empirical relationship for northern California. *Estuaries and Coasts*, 41(7), 2056–2069. https://doi.org/10.1007/S12237-018-0372-0/FIGURES/8

Delgado, J. A., Sudre, J., Tanahara, S., Montes, I., Hernandez-Ayon, J. M., & Zirino, A. (2019). Effect of Caribbean Water incursion into the Gulf of Mexico derived from absolute dynamic topography, satellite data, and remotely sensed chlorophyll a. *Ocean Science, 15*(6), 1561–1578. https://doi.org/10.5194/OS-15-1561-2019

Dickson, A. G. (1990). Standard potential of the reaction: AgCl(s) + 12H2(g) = Ag(s) + HCl(aq), and and the standard acidity constant of the ion HSO4− in synthetic sea water from 273.15 to 318.15 K. *The Journal of Chemical Thermodynamics*, 22(2), 113–127. https://doi.org/10.1016/0021-9614(90)90074-Z

Dickson, A. G., & Millero, F. J. (1987). A comparison of the equilibrium constants for the dissociation of carbonic acid in seawater media. *Deep Sea Research Part A, Oceanographic Research Papers*, 34(10), 1733–1743. https://doi.org/10.1016/0198-0149(87)90021-5

Dickson, A.G., Sabine, C.L. and Christian, J.R. (2007). Guide to Best Practices for Ocean CO2 Measurements. *PICES Special Publication 3*, 191.

Doney, S. C., Fabry, V. J., Feely, R. A., & Kleypas, J. A. (2009). Ocean acidification: The other CO2 problem. *Annual Review of Marine Science, 1*, 169–192. https://doi.org/10.1146/ANNUREV.MARINE.010908.163834

Douglas, N. K., & Byrne, R. H. (2017). Achieving accurate spectrophotometric pH measurements using unpurified meta-cresol purple. *Marine Chemistry*, 190, 66–72. https://doi.org/10.1016/j.marchem.2017.02.004

Duarte, C. M., Hendriks, I. E., Moore, T. S., Olsen, Y. S., Steckbauer, A., Ramajo, L., Carstensen, J., Trotter, J. A., & McCulloch, M. (2013). Is Ocean Acidification an open-ocean syndrome? Understanding anthropogenic impacts on seawater pH. *Estuaries and Coasts, 36*(2), 221–236. https://doi.org/10.1007/S12237-013-9594-3/TABLES/1

Evans, W., Mathis, J. T., Winsor, P., Statscewich, H., & Whitledge, T. E. (2013). A regression modeling approach for studying carbonate system variability in the northern Gulf of Alaska. *Journal of Geophysical Research: Oceans, 118*, 476–489. doi:10.1029/2012JC008246.

Fabry, V. J., Seibel, B. A., Feely, R. A., & Orr, J. C. (2008). Impacts of ocean acidification on marine fauna and ecosystem processes. *ICES Journal of Marine Science, 65*(3), 414–432. https://doi.org/10.1093/ICESJMS/FSN048

Fajar, N. M., García-Ibáñez, M. I., SanLeón-Bartolomé, H., Álvarez, M., & Pérez, F. F. (2015). Spectrophotometric measurements of the carbonate ion concentration: Aragonite saturation states in the Mediterranean Sea and Atlantic Ocean. *Environmental Science and Technology*, 49(19), 11679–11687. https://doi.org/10.1021/ACS.EST.5B03033

Feely, R. A., Sabine, C. L., Hernandez-Ayon, J. M., Ianson, D., & Hales, B. (2008). Evidence for upwelling of corrosive “acidified” water onto the continental shelf. *Science*, *320*(5882), 1490–1492. https://doi.org/10.1126/science.1155676

Fourrier, M., Coppola, L., Claustre, H., D’Ortenzio, F., Sauzède, R., & Gattuso, J.-P. (2020). A regional neural network approach to estimate water-column nutrient concentrations and

carbonate system variables in the Mediterranean Sea: CANYON-MED. *Frontiers in Marine Science, 7*(620). https://doi.org/10.3389/FMARS.2020.00620

Fox, J., & Weisberg, S. (2019). An R Companion to Applied Regression, Third edition. Sage, Thousand Oaks CA. https://socialsciences.mcmaster.ca/jfox/Books/Companion/.

Friedlingstein, P., O'Sullivan, M., Jones, M. W., Andrew, R. M., Hauck, J., Olsen, A., Peters, G.P., Peters, W., Pongratz, J., Sitch, S., Le Quere, C., Canadell, J.G., Ciais, P., Jackson, R.B., Alin, S., Aragao, L.E.O.C., Arnteth, A., Arora, V., Bates, N.R., ... Zaehle, S. (2020). *Global Carbon Budget 2020, Earth Syst. Sci. Data, 12*, 3269–3340. https://doi.org/10.5194/essd-12-3269-2020

García-Ibáñez, M. I., Zunino, P., Fröb, F., Carracedo, L. I., Ríos, A. F., Mercier, H., Olsen, A., & Pérez, F. F. (2016). Ocean acidification in the subpolar North Atlantic: rates and mechanisms controlling pH changes. *Biogeosciences, 13*, 3701–3715. https://doi.org/10.5194/bg-13-3701-2016

Gil-Agudelo, D. L., Cintra-Buenrostro, C. E., Brenner, J., González-Díaz, P., Kiene, W., Lustic, C., & Pérez-España, H. (2020). Coral reefs in the Gulf of Mexico large marine ecosystem: Conservation status, challenges, and opportunities. *Frontiers in Marine Science*, *6*, 807. https://doi.org/10.3389/FMARS.2019.00807/BIBTEX

Goodwin, C., Rodolfo-Metalpa, R., Picton, B., & Hall-Spencer, J. M. (2014). Effects of ocean acidification on sponge communities. *Marine Ecology*, 35(SUPPL1), 41–49. https://doi.org/10.1111/MAEC.12093

Grabowski, J. H., Brumbaugh, R. D., Conrad, R. F., Keeler, A. G., Opaluch, J. J., Peterson, C. H., Piehler, M. F., Powers, S. P., & Smyth, A. R. (2012). Economic valuation of ecosystem

services provided by oyster reefs. *BioScience,* 62(10), 900–909. https://doi.org/10.1525/BIO.2012.62.10.10

Gran, G. (1952). Determination of the equivalence point in potentiometric titrations. Part II. Analyst, 77(920), 661-671.

Hales, B., Takahashi, T., & Bandstra, L. (2005). Atmospheric CO2 uptake by a coastal upwelling system. *Global Biogeochemical Cycles, 19*(1), 1–11. https://doi.org/10.1029/2004GB002295

Hu, X., Nuttall, M. F., Wang, H., Yao, H., Staryk, C. J., McCutcheon, M. R., Eckert, R. J., Embesi, J. A., Johnston, M. A., Hickerson, E. L., Schmahl, G. P., Manzello, D., Enochs, I. C., DiMarco, S., & Barbero, L. (2018). Seasonal variability of carbonate chemistry and decadal changes in waters of a marine sanctuary in the Northwestern Gulf of Mexico. *Marine Chemistry*, *205*(July), 16–28. https://doi.org/10.1016/j.marchem.2018.07.006

Hu, X. (2019). Ocean Acidification studies in the Gulf of Mexico: Current status and future research needs. *Proceedings: The Gulf of Mexico Workshop on International Research*.

Hu, X., Li, Q., Huang, W. J., Chen, B., Cai, W. J., Rabalais, N. N., & Eugene Turner, R. (2017). Effects of eutrophication and benthic respiration on water column carbonate chemistry in a traditional hypoxic zone in the Northern Gulf of Mexico. *Marine Chemistry, 194*, 33–42. https://doi.org/10.1016/j.marchem.2017.04.004

Huang, W.-J., Cai, W.-J., Wang, Y., Hu, X., Chen, B., Lohrenz, S. E., Chakraborty, S., He, R., Brandes, J., & Hopkinson, C. S. (2015). The response of inorganic carbon distributions and dynamics to upwelling-favorable winds on the northern Gulf of Mexico during summer. *Continental Shelf Research*, *111*, 211–222. https://doi.org/10.1016/j.csr.2015.08.020

Ishida, H., Isono, R. S., Kita, J., & Watanabe, Y. W. (2021). Long-term ocean acidification trends in coastal waters around Japan. *Scientific Reports 2021, 11(1)*, 1–7. https://doi.org/10.1038/s41598-021-84657-0

Jiang, L.-Q., Carter, B. R., Feely, R. A., Lauvset, S. K., & Olsen, A. (2019). Surface ocean pH and buffer capacity: Past, present and future. *Scientific Reports 2019, 9*(1), 1–11. https://doi.org/10.1038/s41598-019-55039-4

Jochens, A. E., & DiMarco, S. F. (2008). Physical oceanographic conditions in the deepwater Gulf of Mexico in summer 2000–2002. *Deep Sea Research Part II: Topical Studies in Oceanography, 55*(24–26), 2541–2554. https://doi.org/10.1016/J.DSR2.2008.07.003

Johnson, K. M., A. E. King, and J. McN. Sieburth. 1985. Coulometric TCO2 analyses for marine studies: An introduction. *Marine Chemistry 16*, 61–82.

Johnston MA, Eckert RJ, Sterne TK, Nuttall MF, Hu X, Embesi JA, Hickerson EL, Schmahl GP. 2016. Long-term monitoring at east and west Flower Garden Banks: 2015 annual report. US Marine Sanctuaries Conservation Series ONMS-16-02. Galveston (TX): National Oceanic and Atmospheric Administration, Flower Garden Banks National Marine Sanctuary, US Department of Commerce.

Juranek, L. W., Feely, R. A., Gilbert, D., Freeland, H., & Miller, L. A. (2011). Real-time estimation of pH and aragonite saturation state from Argo profiling floats: Prospects for an autonomous carbon observing strategy. *Geophysical Research Letters*, 38(17), 1–7. https://doi.org/10.1029/2011GL048580

Juranek, L. W., Feely, R. A., Peterson, W. T., Alin, S. R., Hales, B., Lee, K., Sabine, C. L., & Peterson, J. (2009). A novel method for determination of aragonite saturation state on the

continental shelf of central Oregon using multiparameter relationships with hydrographic data. *Geophysical Research Letters, 36*(L24601). doi:10.1029/2009GL040778.

Kim, T. W., Lee, K., Feely, R. A., Sabine, C. L., Chen, C. T. A., Jeong, H. J., & Kim, K. Y. (2010). Prediction of Sea of Japan (East Sea) acidification over the past 40 years using a multiparameter regression model. *Global Biogeochemical Cycles, 24*, GB3005. doi:10.1029/2009GB003637.

Kleypas, J.A., R.A. Feely, V.J. Fabry, C. Langdon, C.L. Sabine, and Robbins L.L. (2006). Impacts of ocean acidification on coral reefs and other marine calcifiers: A guide for future research, report of a workshop held 18–20 April 2005, St. Petersburg, FL, sponsored by NSF, NOAA, and the U.S. Geological Survey, 88pp.

Komyakova, V., Munday, P. L., & Jones, G. P. (2013). Relative importance of coral cover, habitat complexity and diversity in determining the structure of reef fish communities. *PLOS ONE*, 8(12), e83178. https://doi.org/10.1371/JOURNAL.PONE.0083178

Lee, K., Wanninkhof, R., Feely, R. A., Millero, F. J., & Peng, T. H. (2000). Global relationships of total inorganic carbon with temperature and nitrate in surface seawater. Global *Biogeochemical Cycles*, 14(3), 979–994. https://doi.org/10.1029/1998GB001087

Liu, X., Patsavas, M. C., & Byrne, R. H. (2011). Purification and characterization of meta-cresol purple for spectrophotometric seawater pH measurements. *Environmental Science and Technology, 45*(11), 4862–4868. https://doi.org/10.1021/es200665d

Liu, P. J., Ang, S. J., Mayfield, A. B., & Lin, H. J. (2020). Influence of the seagrass Thalassia hemprichii on coral reef mesocosms exposed to ocean acidification and experimentally elevated temperatures. *Science of The Total Environment*, *700*, 134464. https://doi.org/10.1016/J.SCITOTENV.2019.134464

Madin, J. S., O'Donnell, M. J., & Connolly, S. R. (2008). Climate-mediated mechanical changes to post-disturbance coral assemblages. *Biology Letters, 4*(5), 490–493. https://doi.org/10.1098/%2Frsbl.2008.0249.

McGarry, K., Siedlecki, S. A., Salisbury, J., & Alin, S. R. (2021). Multiple linear regression models for reconstructing and exploring processes controlling the carbonate system of the northeast US from basic hydrographic data. *Journal of Geophysical Research: Oceans, 126*(2), e2020JC016480. https://doi.org/10.1029/2020JC016480

Mehrbach, C., Culberson, C. H., Hawley, J. E., & Pytkowicx, R. M. (1973). Measurement of the apparent dissociation constants of carbonic acid in seawater at atmospheric pressure. *Limnology and Oceanography*, 18(6), 897–907. https://doi.org/10.4319/LO.1973.18.6.0897

Miller, J. R., & Russell, G. L. (1992). The impact of global warming on river runoff. Journal of *Geophysical Research*, 97(D3), 2757–2764. https://doi.org/10.1029/91JD01700

Milliman, J. D., Farnsworth, K. L., Jones, P. D., Xu, K. H., & Smith, L. C. (2008). Climatic and anthropogenic factors affecting river discharge to the global ocean, 1951–2000. Global and *Planetary Change*, 62(3–4), 187–194. https://doi.org/10.1016/J.GLOPLACHA.2008.03.001

Morey, S. L., Schroeder, W. W., O'Brien, J. J., & Zavala-Hidalgo, J. (2003). The annual cycle of riverine influence in the eastern Gulf of Mexico basin. *Geophysical Research Letters, 30*(16). https://doi.org/10.1029/2003GL017348

Mucci, A. (1983). The solubility of calcite and aragonite in seawater at various salinities, temperatures, and one atmosphere total pressure. *American Journal of Science*, 283, 780–799. https://www.ajsonline.org/content/ajs/283/7/780.full.pdf

Muller-Karger, F. E., Smith, J. P., Werner, S., Chen, R., Roffer, M., Liu, Y., Muhling, B., Lindo-Atichati, D., Lamkin, J., Cerdeira-Estrada, S., & Enfield, D. B. (2015). Natural variability of

surface oceanographic conditions in the offshore Gulf of Mexico. *Progress in Oceanography, 134*, 54–76. https://doi.org/10.1016/J.POCEAN.2014.12.007

Munday, P. L., Gagliano, M., Donelson, J. M., Dixson, D. L., & Thorrold, S. R. (2011a). Ocean acidification does not affect the early life history development of a tropical marine fish. *Marine Ecology Progress Series*, 423, 211–221. https://doi.org/10.3354/MEPS08990

Munday, P. L., Hernaman, V., Dixson, D. L., & Thorrold, S. R. (2011b). Effect of ocean acidification on otolith development in larvae of a tropical marine fish. *Biogeosciences*, 8(6), 1631–1641. https://doi.org/10.5194/BG-8-1631-2011

Narita, D., Rehdanz, K., & Tol, R. S. J. (2012). Economic costs of ocean acidification: A look into the impacts on global shellfish production. *Climatic Change*, 113(3–4), 1049–1063. https://doi.org/10.1007/S10584-011-0383-3/FIGURES/4

Oey, L. Y., Ezer, T., & Lee, H. C. (2005). Loop Current, rings and related circulation in the Gulf of Mexico: A review of numerical models and future challenges. *Geophysical Monograph, 161*, 31–56.

Orr, J. C., Epitalon, J. M., Dickson, A. G., & Gattuso, J. P. (2018). Routine uncertainty propagation for the marine carbon dioxide system. *Marine Chemistry*, *207*, 84–107. https://doi.org/10.1016/J.MARCHEM.2018.10.006

Orr, J. C., Fabry, V. J., Aumont, O., Bopp, L., Doney, S. C., et al. (2005). Anthropogenic ocean acidification over the twenty-first century and its impact on calcifying organisms, *Nature, 437*:681–86. https://doi.org/10.1038/nature04095.

Peng, T.-H., & Langdon, C. (2007). *Gulf of Mexico and East Coast Carbon Cruise (GOMECC) Chief Scientists: Tsung-Hung Peng and Chris Langdon NOAA Atlantic Oceanographic and Meteorological Laboratory Cruise Report*

Perry, C. T., Murphy, G. N., Kench, P. S., Smithers, S. G., Edinger, E. N., Steneck, R. S., & Mumby, P. J. (2013). Caribbean-wide decline in carbonate production threatens coral reef growth. *Nature Communications, 4*(1402). https://doi.org/10.1038/ncomms2409

Portela, E., Tenreiro, M., Pallàs-Sanz, E., Meunier, T., Ruiz-Angulo, A., Sosa-Gutiérrez, R., & Cusí, S. (2018). Hydrography of the central and western Gulf of Mexico. *Journal of Geophysical Research: Oceans*, 123(8), 5134–5149. https://doi.org/10.1029/2018JC013813

Porzio, L., Buia, M. C., & Hall-Spencer, J. M. (2011). Effects of ocean acidification on macroalgal communities. *Journal of Experimental Marine Biology and Ecology*, 400(1–2), 278–287. https://doi.org/10.1016/J.JEMBE.2011.02.011

Quinn, G. P., & Keough, M. J. (2002). *Experimental Design and Data Analysis for Biologists,* Cambridge University Press. www.cambridge.org/97805211800286

Rabalais, N. N., Turner, R. E., Díaz, R. J., Justic´rabalais, D., Justic´rabalais, J., Turner, N. N., Díaz, R. E., Justic´, J., Rabalais, N. N., Turner, R. E., & Justic´:, D. (2009). Global change and eutrophication of coastal waters. *ICES Journal of Marine Science*, 66(7), 1528–1537. https://doi.org/10.1093/ICESJMS/FSP047

Rabalais, N. N., Turner, R. E., & Scavia, D. (2002). Beyond science into policy: Gulf of Mexico hypoxia and the Mississippi River. *BioScience*, 52(2), 129–142. https://doi.org/10.1641/0006-3568(2002)052[0129:BSIPGO]2.0.CO;2

Roemmich, D., Alford, M. H., Claustre, H., Johnson, K. S., King, B., Moum, J., Oke, P. R., Owens, W. B., Pouliquen, S., Purkey, S., Scanderbeg, M., Suga, T., Wijffels, S. E., Zilberman, N., Bakker, D., Baringer, M. O., Belbeoch, M., Bittig, H. C., Boss, E., … Yasuda, I. (2019). On the future of Argo: A global, full-depth, multi-disciplinary array.

Frontiers in Marine Science, *6*(JUL), 439. https://doi.org/10.3389/FMARS.2019.00439/BIBTEX

Sabine, C. L., Feely, R. A., Gruber, N., Key, R. M., Lee, K., Bullister, J. L., Wanninkhof, R., Wong, C. S., Wallace, D. W. R., Tilbrook, B., Millero, F. J., Peng, T. H., Kozyr, A., Ono, T., & Rios, A. F. (2004). The oceanic sink for anthropogenic CO_2. *Science, 305*(5682), 367–371. https://doi.org/10.1126/science.1097403.

Sahoo, S., & Pandey, S. (2020). Bibliometric analysis and visualization of global ocean acidification research. *Science and Technology Libraries, 39*(4), 414–431. https://doi.org/10.1080/0194262X.2020.1776194.

Salisbury, J., Green, M., & Hunt, C. (2008). Coastal acidification by rivers: A threat to shellfish? *EOS, 89*(50), 513.

Schneider, K., & Erez, J. (2006). The effect of carbonate chemistry on calcification and photosynthesis in the hermatypic coral Acropora eurystoma. *Limnology and Oceanography, 51*(3), 1284–1. https://doi.org/10.4319/lo.2006.51.3.1284.

Seelmann, K., Abmann, S., & Körtzinger, A. (2019). Characterization of a novel autonomous analyzer for seawater total alkalinity: Results from laboratory and field tests. *Limnology and Oceanography: Methods, 17*(10), 515–532. https://doi.org/10.1002/LOM3.10329

Snyder, M. A., Sloan, L. C., Diffenbaugh, N. S., & Bell, J. L. (2003). Future climate change and upwelling in the California Current. *Geophysical Research Letters, 30*(15). https://doi.org/10.1029/2003GL017647

Sturges, W., & Leben, R. (2000). Frequency of ring separations from the Loop Current in the Gulf of Mexico: A revised estimate. *Journal of Physical Oceanography, 30*(7), 1814–1819. https://doi.org/10.1175/1520-0485(2000)0302.0.CO;2

Sunda, W. G., & Cai, W. J. (2012). Eutrophication induced CO2-acidification of subsurface coastal waters: Interactive effects of temperature, salinity, and atmospheric P CO2. *Environmental Science and Technology*, 46(19), 10651–10659. https://doi.org/10.1021/ES300626F/SUPPL_FILE/ES300626F_SI_001.PDF

Takahashi, M., Noonan, S. H. C., Fabricius, K. E., & Collier, C. J. (2016). The effects of long-term in situ CO2 enrichment on tropical seagrass communities at volcanic vents. ICES *Journal of Marine Science*, 73(3), 876–886. https://doi.org/10.1093/ICESJMS/FSV157

Takeshita, Y., Johnson, K. S., Martz, T. R., Plant, J. N., & Sarmiento, J. L. (2018). Assessment of autonomous pH measurements for determining surface seawater partial pressure of CO_2. *Journal of Geophysical Research: Oceans, 123*(6), 4003–4013. https://doi.org/10.1029/2017JC013387

Testor, P., DeYoung, B., Rudnick, D. L., Glenn, S., Hayes, D., Lee, C., Pattiaratchi, C. B., Hill, K. L., Heslop, E., Turpin, V., Alenius, P., Barrera, C., Barth, J., Beaird, N., Becu, G., Bosse, A., Bourrin, F., Brearley, A., Chao, Y., … Wilson, D. (2019). OceanGliders: A component of the integrated GOOS. *Frontiers in Marine Science*, *6*(JUL), 422. https://doi.org/10.3389/FMARS.2019.00422/BIBTEX

Uppström, L. R., Uppström, & R., L. (1974). The boron/chlorinity ratio of deep-sea water from the Pacific Ocean. *DSRA*, 21(2), 161–162. https://doi.org/10.1016/0011-7471(74)90074-6

van Heuven, S., D. Pierrot, J.W.B. Rae, E. Lewis, and Wallace, D.W.R. (2011). MATLAB program developed for CO_2 system calculations. Carbon Dioxide Information Analysis Center, Oak Ridge National Laboratory, U.S. Department of Energy, Oak Ridge, Tennessee. doi: 10.3334/CDIAC/otg.CO2SYS_MATLAB_v1.1

Velez, Z., Costa, R. A., Wang, W., & Hubbard, P. C. (2021). Independent effects of seawater pH and high P CO 2 on olfactory sensitivity in fish: possible role of carbonic anhydrase. *Journal of Experimental Biology*. doi: 10.1242/jeb.238485.

Vidal, V. M. V., Vidal, F. V., Hernandez, A. F., Meza, E., & Perez- Molero, J. M. (1994). Baroclinic flows, transports, and kinematic properties in a cyclonic-anticyclonic-cyclonic ring triad in the Gulf of Mexico. *Journal of Geophysical Research: Oceans, 99*(C4), 7571–7597. https://doi.org/10.1029/93JC03334

Vidal, V. M. V, Vidal, F. V, & Perez-Molero, J. M. (1992). Collision of a loop current anticyclonic ring against the continental shelf slope of the western Gulf of Mexico. *Journal of Geophysical Research: Oceans, 97*(C2), 2155–2172. https://doi.org/10.1029/91JC00486

Wallace, R. B., Baumann, H., Grear, J. S., Aller, R. C., & Gobler, C. J. (2014). Coastal ocean acidification: The other eutrophication problem. *Estuarine Coastal and Shelf Science*, 148, 1–13. https://doi.org/10.1016/J.ECSS.2014.05.027

Wanninkhof, R., Wood, M., & Barbero, L. (2012). Gulf of Mexico and East Coast Carbon Cruise #2 (GOMECC-2). *NOAA Atlantic Oceanographic and Meteorological Laboratory*. http://www.aoml.noaa.gov/ocd/gcc/GOMECC2/

Winkler, L. W. (1888): Die Bestimmung des im Wasser gelesten Sauerstoffen. *Ber. Dtsche. Chem. Ges., 21*, 2843-2855.

Wood, H.L., Spicer, J.I. & Widdicombe, S. (2008). Ocean acidification may increase calcification rates, but at a cost. *Proceeding of the Royal Society B, 275*, 1767–1773.

Yang, B., Gao, X., & Xing, Q. (2018). Geochemistry of organic carbon in surface sediments of a summer hypoxic region in the coastal waters of northern Shandong Peninsula. *Continental Shelf Research*, *171*, 113–125. https://doi.org/10.1016/J.CSR.2018.10.015

Zavala-Hidalgo, J., Gallegos-García, A., Martínez-López, B., Morey, S. L., & O'Brien, J. J. (2006). Seasonal upwelling on the western and southern shelves of the Gulf of Mexico. *Ocean Dynamics*, *56*(3–4), 333–338. https://doi.org/10.1007/S10236-006-0072-3/FIGURES/7

Zakroff, C. J., & Mooney, T. A. (2020). Antagonistic interactions and clutch-dependent sensitivity induce variable responses to ocean acidification and warming in squid (Doryteuthis pealeii) embryos and paralarvae. *Frontiers in Physiology 11*(501). doi:10.3389/fphys.2020.00501.

Zeebe, R. E., & Wolf-Gladrow, D. (2001). CO_2 in Seawater: Equilibrium, Kinetics, Isotopes, Volume 65 - 1st Edition. Elsevier Science. https://www.elsevier.com/books/co2-in-seawater-equilibrium-kin

Zimmerman, R. C. (2021). Scaling up: Predicting the impacts of climate change on seagrass ecosystems. *Estuaries and Coasts*, 44, 558–567. https://doi.org/10.1007/s12237-020-00837-7/Published